mathematics

MDPI

Article

Optimized Sizing of Energy Management System for Off-Grid Hybrid Solar/Wind/Battery/Biogasifier/Diesel Microgrid System

Ali M. Jasim [1,2,*], Basil H. Jasim [1], Florin-Constantin Baiceanu [3,*] and Bogdan-Constantin Neagu [3,*]

[1] Electrical Engineering Department, University of Basra, Basra 61001, Iraq
[2] Department of Communications Engineering, Iraq University College, Basra 61001, Iraq
[3] Power Engineering Department, Gheorghe Asachi Technical University of Iasi, 700050 Iasi, Romania
* Correspondence: e.alim.j.92@gmail.com (A.M.J.); florin.baiceanu@tuiasi.ro (F.-C.B.); bogdan.neagu@tuiasi.ro (B.-C.N.)

Abstract: Recent advances in electric grid technology have led to sustainable, modern, decentralized, bidirectional microgrids (MGs). The MGs can support energy storage, renewable energy sources (RESs), power electronics converters, and energy management systems. The MG system is less costly and creates less CO_2 than traditional power systems, which have significant operational and fuel expenses. In this paper, the proposed hybrid MG adopts renewable energies, including solar photovoltaic (PV), wind turbines (WT), biomass gasifiers (biogasifier), batteries' storage energies, and a backup diesel generator. The energy management system of the adopted MG resources is intended to satisfy the load demand of Basra, a city in southern Iraq, considering the city's real climate and demand data. For optimal sizing of the proposed MG components, a meta-heuristic optimization algorithm (Hybrid Grey Wolf with Cuckoo Search Optimization (GWCSO)) is applied. The simulation results are compared with those achieved using Particle Swarm Optimization (PSO), Genetic Algorithms (GA), Grey Wolf Optimization (GWO), Cuckoo Search Optimization (CSO), and Antlion Optimization (ALO) to evaluate the optimal sizing results with minimum costs. Since the adopted GWCSO has the lowest deviation, it is more robust than the other algorithms, and their optimal number of component units, annual cost, and Levelized Cost Of Energy (LCOE) are superior to the other ones. According to the optimal annual analysis, LCOE is 0.1192 and the overall system will cost about USD 2.6918 billion.

Keywords: islanded microgrid; energy management system; renewable energy sources; grey wolf optimization; cuckoo search; optimal sizing; levelized cost of energy

MSC: 91B74; 68W50

Citation: Jasim, A.M.; Jasim, B.H.; Baiceanu, F.-C.; Neagu, B.-C. Optimized Sizing of Energy Management System for Off-Grid Hybrid Solar/Wind/Battery/Biogasifier/Diesel Microgrid System. *Mathematics* **2023**, *11*, 1248. https://doi.org/10.3390/math11051248

Academic Editor: Duarte Valério

Received: 22 January 2023
Revised: 16 February 2023
Accepted: 1 March 2023
Published: 4 March 2023
Corrected: 8 April 2024

1. Introduction

Currently, fossil fuels are used to generate the majority of the world's electricity. Fast depletion rates and severe environmental impacts caused by the combustion process are the main drawbacks of these resources. Since fossil fuels are being consumed quickly around the world, there is an urgent need to find other sources of energy to meet the current demand. RESs can be derived from a variety of sources, including solar, wind, tidal, biomass, other alternative non-polluting and sustainable energy sources. Since they are non-polluting and long-lasting, RESs are poised to become the dominant form of electricity production in the near future [1–6]. Sizing these resources is key to making their systems economical and reliable. MGs are under- or oversized to satisfy electricity demands. An oversized systems will incur high running expenses and produce excess energy. In contrast, an inadequately scaled MG system will be unable to deliver power to the necessary demands. To fully reap the advantages of a RES-based MG, optimal size and energy management are needed. RESs have a considerably larger chance of succeeding

in cities where a huge population still exceeds the electricity generating capacity of a centralized grid [7].

Iraq's electricity sector is facing multiple problems at once. Power generation in Iraq has increased from 5 GW in 2005 to a peak usage of 19.2 GW in 2020 [8]. This is due in large part to the country's recent efforts to restore its aging power infrastructure. Unfortunately, the electricity industry is still plagued by over 10% annual demand growth and significant transmission and distribution losses. However, because of the peak demand and increased consumption, particularly in the summer, the country frequently imports from surrounding countries. Strategically located in the world's solar belt, Iraq is fortunate to receive more than 3000 h of bright sunlight per year, with an average daily sunshine duration of 11 × 1012 h in summer and 7 × 108 h in winter.

This study is applied in Basra, a city in southern Iraq that has the following geographical coordinates: latitude: 30°30′30″ N, longitude: 47°46′49″ E, and elevation above sea level: 4 m = 13 ft [9]. The daily maximum solar radiation in Basra varies from 965 W/m^2 in December to 1040 W/m^2 in August. The majority of countries in the world receive fewer daylight hours in a day than Iraq [9,10]. Moreover, during the winter in Iraq, sunny days still produce more sunshine than cloudy and rainy days [11]. One-sixth of the nation has a yearly wind speed greater than 5 m per second, according to reference [12]. A significant amount of Iraq's electricity needs could be met by wind farms. The wind speed in Basra can reach 10 m/s or more. According to the reference [13], the preferred area for both wind and solar energy is Basra. Based on the findings, Basra produced the most solar energy, followed by Mosul and Baghdad. When it comes to the energy produced by wind turbines, Basra leads the pack, followed by Mosul and Baghdad. With its abundance of fossil fuels, Iraq is still a major player in the global energy market [14]. It is for this reason that solar power is not popular with Iraq's ruling elite. Therefore, neither the Iraqi government nor the Iraqi people appreciate the significance of renewable energy. Consequently, the development of renewable energy technology is essential and can only be accomplished via the efforts of interested persons and non-governmental groups, as opposed to official policy. In the past years, the energy problem has grown increasingly complex. Energy shortages have emerged in Iraq despite the country's substantial fossil fuel supplies because of the widespread destruction that occurred there in 1991. In addition, fossil fuel reserves are dwindling and are likely to be depleted within the next century. In this situation, renewable power is the only reliable source of energy that will also aid in lowering CO_2 emissions from conventional and alternative fuels. This climatic benefit of solar and wind energy should prompt its rapid consideration, since it can assist in offsetting the impacts of global warming [15,16].

Several researchers report hybrid MGs. The hybrid energy system is not a new idea, but it has recently received more attention from researchers. In [17], just a WT and battery-backed PV generation were explored, and in [18], a diesel generator was included as a backup. A number of studies have been conducted to determine the best method for optimizing the setup of hybrid systems. For the optimum sizing of an autonomous photovoltaic/wind/battery/diesel generator MG system, the Grasshopper Optimization Algorithm (GOA) is applied as a metaheuristic optimization method [19]. Particle swarm optimization and the Cuckoo Search (CS) optimization algorithm's performance are compared to the suggested GOA's efficacy in addressing the optimization problem. For the optimum sizing of a standalone hybrid solar and wind energy system, a hybrid optimization technique based on three algorithms—chaotic search, harmony search, and simulated annealing (SA)—was developed in [20]. The authors in [21] used a fuzzy logic-based model to reduce the yearly cost of a PV–WT–battery hybrid system. Using GA in conjunction with an energy management approach, the authors of [22] presented a method for efficiently determining the optimal size of the hybrid WT–PV–battery system's component. In order to minimize the total net price and LCOE, the author of [23] employed GWO to figure out what size WT–PV–biomass system would operate optimally. By comparing the GWO method's outcomes to those of GA and SA, it was found that the former was more effective.

With the help of the Bonobo optimization method based on annual cost reduction, the optimal size of a WT–PV–battery–diesel microgrid was found in [24]. Reference [25] proposes a new method integrating a crow search algorithm (CSA) for optimizing the scale of a HRES in a remote area. The system includes PV panels, wind turbines, diesel generators (DGs), and batteries. The goal is to use renewable energy sources cost-effectively (RESs). The CSA is simple to implement, requires few parameters, and is flexible. It compared the results to the elephant herding optimizer (EHO), grasshopper optimization algorithm (GOA), Harris hawks optimizer (HHO), seagull optimization algorithm (SOA), and spotted hyena optimizer (SHO) approaches (SHO). This optimization method had been compared to big-bang–big-crunch (BBBC), crow search (CS), the genetic algorithm (GA), and the butterfly optimization algorithm (BOA) for robustness tests. Using the HOMER software, the authors of [26] investigated the viability of a combined dispatch (CD) control approach for a PV–diesel–battery hybrid system. The results demonstrate that significant effects are exerted on the performance of the proposed system by differences in critical parameters such as time step, battery minimum state of charge, diesel price, solar radiation, and load growth. The hybrid MG system's size was optimized by [27] using PSO. The authors of [28] proposed a brand-new optimization algorithm called Smell Agent Optimization (SAO) to replicate the intelligent actions of an agent pursuing the source of a smell's molecules. The concept, which is divided into three parts (Sniffing, Trailing, and Random), is original and easy to use. The SAO is implemented on 37 CEC benchmark functions and engineering challenges related to hybrid renewable energy systems (HRES), and the results are compared with other meta-heuristic algorithms. Comparatively to the benchmarked algorithms, the statistical findings demonstrated that the SAO also produced the most cost-effective HRES design. Some studies are considered actual case studies. In [29], a PV plant, WT plant, storage units, and diesel generators hybrid arrangement was created by an in-depth assessment of the available options. In order to evaluate the planned configurations and find the ideal configuration integrating conventional and renewable energy sources, a case study in Egypt has been taken into consideration. With a LCOE of 0.124 USD/kWh, the findings reveal that the linked power grid with PV-diesel generators with no storage devices is the most effective design. MG planning steps for Vietnam's Con Dao Island have been detailed in [30]. Many optimization techniques have been suggested and implemented to find the best MG configurations outside of the predetermined configurational platforms. Efforts to propose a strategy for optimizing the size of ultracapacitor-battery hybrid storage systems have been developed, and are usefully presented in [31]. This method has applications in both smart grids and plug-in electric automobiles. The suggested energy management strategy, built on a Markov chain and a stochastic dynamic programming (SDP) algorithm, has been used in practical settings. In addition, an Egyptian hamlet has been selected as a representative example. To meet the need for power, engineers have created a comprehensive system that combines WT–PV–diesel generators–battery storage units [32]. Model-predictive control (MPC) and GA provide a LCOE of 0.123 USD/kWh [33] for a PV–WT–biomass–H2–fuel cell hybrid system in Spain. An optimized MG layout for a hybrid PV–FC–battery system was presented in this study [34]. Considered is a real-world case study in Egypt's Dobaa area involving the emergency supply of safety loads at a nuclear power station, with load characteristics and geographical data taken into account. In this research, the authors used and compared the optimization methods of the equilibrium optimizer (EQ), the black-hole-based optimization (BHB), and the bat optimization (BAT). A nearby town in Thailand with a peak demand of roughly 76 kW was the subject of paper [35], which offered an overall system and topology MG design. Without the need for human intervention, the system could run and be maintained. Focusing on component sizing, the research [36] aims to develop a hybrid system for a port MG. The Port of Aalborg in Denmark has been chosen as the case study location. The planned grid-connected building has solar panels, wind turbines, a battery bank, and cold-ironing equipment. Economic viability, energy reliability, and environmental implications are then assessed to determine the optimal arrangement. A standalone MG power system is suggested in [37] to electrify a small

agricultural settlement in Palestinian territory. Residential and water pumps are included. The village has 30 houses and a water pumping infrastructure. The typical load requires 300 kWh/day and 12.5 kW. Water pumping uses 49 kWh/day. Daily sun radiation averages 5.6 kWh/m^2 in the area. The finest hybrid system is a PV with battery storage paired with a diesel generator. The PV–biomass system for a farm and nearby residential neighborhood in the Pakistani region of Pinjab was described and optimized in paper [38]. Sensitivity analysis was used to fine-tune the NPV and COE estimates. It factored in the availability of biomass, the cost of biomass, the amount of solar radiation, and the fluctuation of the load. Using a variant of the cascade analysis approach for electric systems, the author of [39] offered a design for a hybrid generating system. A MATLAB/Simulink model was utilized for simulation, and the findings were verified by means of the HOMER program. Decentralized hybrid systems in Sabah, Malaysia, were evaluated for their technical, economic, and environmental performance by the authors of [40]. In order to evaluate the effects of PV integration, several penetration rates were taken into account. The NPV and LCOE were optimized, and a sensitivity study was conducted. PV–DG–ESS not only performed well economically and environmentally, but also technically. An economic feasibility study of a PV/WT system for a typical house in Dubai, UAE, is performed in [41]. Return on investment was computed using several assumptions for inputs such as power price and interest rate. The results reveal that the suggested method became unfeasible at an annual interest rate of more than 8%. In order to meet the 350 kWh/day load demand in a rural area of Bangladesh, [42] analyzes the performance of a PV–diesel–battery system in a stand-alone hybrid application. The study [43] models a MG system using solar photovoltaic, wind, and storage batteries in Bahir Dar, Ethiopia. Continuous power delivery to the load requires a storage or grid system. The system was created to supply the city's load demand reliably and with acceptable power quality, something conventional generating alone cannot do. Residential, commercial, institutional, agricultural, and small manufacturing loads average 15,467 KWh/day. HOMER pro software is used to size MG system components optimally. Size optimization for PV–MHP-based hybrid power systems in rural Himachal Pradesh, India, has been explored by Kumar et al. [44]. Table 1 summarizes the optimal sizing of MG renewable energy systems based on energy management strategy, cost analysis, algorithm comparison, robustness, and speed tests.

Table 1. Previous studies considered a taxonomy of optimal sizing of microgrid renewable energy systems considering energy management strategy, cost analysis, reported algorithm comparison, robustness, and speed tests.

Ref. No.	Year	Electrical Resources	Algorithm(s)	Dispatch Operation Strategy	Comprehensive Cost Aanalysis	Compared to Reported Algorithms	Robustness and Speed Tests
[17]	2018	PV–wind–battery	HOMER	NO	NO	NO	NO
[18]	2020	PV–wind–diesel	Heuristic approximation of the Gradient Descent	NO	NO	NO	NO
[19]	2019	PV–wind-battery–diesel	GOA	YES	YES	CS and PSO	NO
[20]	2019	Solar–wind–hydrogen energy	chaotic search, harmony search and simulated annealing	YES	YES	NO	NO
[21]	2018	Photovoltaic–wind–battery s	Fuzzy Inference System	YES	YES	NO	NO
[22]	2019	PV–wind–FC–battery	economic MPC and GA	YES	YES	NO	NO
[23]	2019	PV–WT–biomass	GWO	NO	YES	GA and SA	NO
[24]	2022	PV–wind–battery–diesel	bonobo optimizer	YES	YES	BBBC, CS, GA, and BOA	Robustness test
[25]	2022	PV–wind–battery–diesel	CSA	YES	YES	EHO, GOA, HHO, SOA, and SHO	Robustness test
[26]	2019	PV–diesel–battery	HOMER	YES	YES	NO	NO

Table 1. *Cont.*

Ref. No.	Year	Electrical Resources	Algorithm(s)	Dispatch Operation Strategy	Comprehensive Cost Aanalysis	Compared to Reported Algorithms	Robustness and Speed Tests
[27]	2017	PV–wind–battery–diesel	PSO	NO	YES	NO	NO
[28]	2021	PV–wind–battery	SAO	NO	YES	YES	YES
[29]	2020	PV–battery–diesel	HOMER	YES	YES	NO	NO
[30]	2021	PV–battery–diesel	HOMER	NO	YES	NO	NO
[31]	2019	Battery/ultra-capacitor	Dynamic programming algorithm	NO	NO	NO	NO
[32]	2019	PV–wind–battery–diesel	WOA, WCA, MFO, and PSOGSA	YES	YES	YES	Robustness test
[33]	2019	PV–wind–biomass–H2	MPC and GA	YES	YES	NO	NO
[34]	2022	PV–FC–battery	EQ, BAT, and BHB	YES	YES	YES	Robustness test
[35]	2019	PV–battery	NA	NO	NO	NO	NO
[36]	2022	PV–wind–battery	HOMER	NO	YES	NO	NO
[37]	2020	PV–battery–diesel	HOMER	NO	YES	NO	NO
[38]	2017	Solar–biomass	HOMER	NO	YES	NO	NO
[39]	2016	PV–wind–battery	HOMER	YES	YES	NO	NO
[40]	2017	PV–battery–diesel	HOMER	YES	YES	NO	NO
[41]	2016	PV–wind	HOMER	NO	NO	NO	NO
[42]	2018	PV–battery–diesel	HOMER	YES	YES	NO	NO
[43]	2020	PV–wind–battery	HOMER	NO	YES	NO	NO
[44]	2019	PV–micro-hydro–diesel–battery	PSO	NO	YES	NO	NO

1.1. Global Prospects for Renewable Power Stations and Investment Costs

There are several renewable power plants constructed in various countries at varying costs. According to the study [45], the cost of constructing 1.1 GW of wind power capacity in Africa is expected to be USD 1.8 billion, with development finance institutions contributing 59 percent. Saga Energy of Norway has agreed to invest USD 2.9 billion in a state-owned Iranian firm called Amin Energy to build around 2 GW of solar power facilities in Iran over the next five years. Scatec Solar, a Norwegian solar energy company, has said it is in discussions to create a 110 MW solar project for USD 132 million, with the possibility of expanding the project to 500 MW [46]. In Iran, the Mahan Solar Power Station has the potential to generate 20 MWh per day. This power plant has a total of 76,912 solar panels installed, with roughly 21,000 bases hammered, and the amount of investment is USD 27 million [47]. The same paper demonstrated that in the provinces of Fars, Kerman, and Isfahan, solar energy has the ability to provide the demands of industry and agriculture. A 10 MW solar station facility in Sirjan would require around USD 16.14 million, according to an economic analysis. In order to create more than 2 GW of renewable wind generation and 50 MW of solar electricity generation in Iowa, United States, MidAmerican Energy says it intends to spend USD 3.9 billion [48]. Turkey's energy needs are predicted to double by 2023. Thus, Turkey's 2023 strategy includes ambitious renewable energy ambitions. The Ministry of National Resources and Energy intends to increase the renewable energy capacity to 61,000 MW by 2023. The hydroelectric capacity will be 34,000 MW, wind capacity 20,000 MW, geothermal capacity 1000 MW, solar capacity 5000 MW, and biomass capacity 1000 MW. This will cost over USD 60 billion [49]. Photovoltaic power units at Pakistan's Quaid-e-Azam Solar Park are among China Pakistan Economic Corridor's 14 priority energy projects. The 4500-acre project has a 1000 MW capacity and costs approximately USD 1.50 billion [50]. Mohammed bin Rashid Al Maktoum's solar project is the largest solar park in the world, with a total area of 77 km^2 at Seih Al-Dahal, approximately 50 km south of Dubai. The Dubai Electricity and Water Authority (DEWA) created this undertaking. It is anticipated to have a 5000 MW output capacity by 2030, with total cost of up to 50 billion AED (USD 13.6 billion). When finished, this solar building project will reduce CO_2 emissions by more than 6.5 M tons annually [51,52].

1.2. Research Gap and Contributions

The aforementioned studies in the literature have not explicitly outlined specific design approaches, and some of the proposed design methodologies [18,20,22,23,31–34] are quite complex. To date, no exhaustive evaluations on the techno-economic assessment of WT–PV–battery–diesel generator–bio-gasifier hybrid systems have been conducted. Additionally, the absence of dispatch strategies in such MG optimization and management systems, which are necessary to ensure technical and economic feasibility. Moreover, focusing on a hybrid WT–PV–battery system or the system with a diesel-based backup may still leave a gap between the supply and demand or lead to high total system annual costs, respectively. MG design decisions must be based on a variety of technical, environmental, and financial factors. Taking advantage of RESs may lower installation costs for power plants, utilities, and responsible governments while also lowering CO_2 emissions and electricity rates for end-users. According to the available literature, this work is one of the earliest attempts to use GWCSO algorithm for the optimal design of a stand-alone MG. However, no effort has been made to provide a comprehensive comparison of the performance of the adopted GWCSO algorithm with other ones, including PSO, GA, CSO, GWO, and ALO, to optimize the size of such a hybrid energy system. An actual case study is investigated to assess the feasibility of employing these techniques to develop the hybrid energy system based on tech-economic and eco-indicators. This feasible renewable energy-based MG system is utilized in Basra, Iraq, using real weather and load data. A sensitivity analysis has been conducted to assess the economic and operational effectiveness of the hybrid system in response to variations in certain factors. These factors include the real interest rate, the climate data-based renewable energy (solar irradiance, temperature, and wind speed), the capacity shortage, and the battery's minimal state of charge (SOC). In addition, statistical analyses have been carried out to assess the stability of the implemented algorithms. Specifically, this paper makes the following contributions:

1. This study proposes an optimal size for the energy management MG system in Basra, Iraq, based on renewable, storage, and backup nonrenewable energy sources. This system includes a brand-new hybrid MG system with WT, PV, batteries, a diesel generator, and a biogasifier to address the unreliability of power in off-grid areas. Several aspects of the proposed system's mathematical modeling, including its components and operational processes, have been discussed in detail.
2. In this study, GWCSO algorithm is used. With this algorithm, the optimal component sizes for the system can be determined, resulting in the lowest yearly cost and LCOE. To the best of our knowledge, the sizing of such system components has not previously been determined by combining GWO and CS for an islanded MG.
3. The GWCSO cost analysis results have been compared to the GA, PSO, CS, GWO, and ALO algorithms to determine the most cost-effective one.
4. This study illustrates the techno-economic and environmental consequences of islanded hybrid MG systems at various integration levels by reducing the total number of used components and prioritizing renewables units to meet power demands, making it easier for investors to choose the best system for their investment objectives.

1.3. Research Organization

The remaining sections of this paper are structured as described below. The problem statement is presented in Section 2. In the third section, a general description of the system is given. The proposed system is modeled mathematically in Section 4. A technique for optimization is presented in Section 5. The discussion of objective functions and economic modeling can be found in Section 6. The results of the simulation were presented and discussed in Section 7. In the end, the conclusions of this study are presented in the Section 8.

2. Problem Statement

Basra's power system is centralized and relies on five stations, one of which is thermal, and the others are natural gas, as shown in Figure 1 [53]. It participates in and is connected to the Iraqi network. Annually, with non-RERs, costs may be paid to cover operating and fuel expenses. This causes the network to face a number of challenges. Pollution and CO_2 emissions can be generated from non-renewable stations, which are not adopted here as the paper focuses on simulating suggested RER-based off-grid MG to fulfill the load profile using the MATLAB-based optimal management of adopted energy sources without studying the power stations of the city, their associated costs, or any other data.

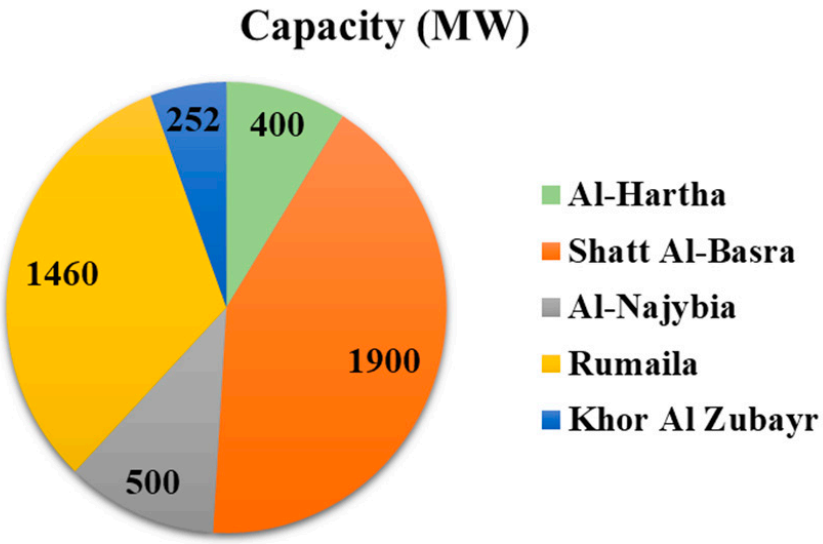

Figure 1. Basra conventional power plants [53].

According to the fuel and operation costs of gas turbines and thermal power stations in Table 2 [8], the necessary annual cost to fulfill a specific consumption (e.g., the annualized load of the city in 2022) may be costly in terms of fuel and operation costs. This describes that the above stations are connected to the centralized network; they may incur heavy costs and cause CO_2 emissions. To lower costs (which are here based on assumption values), CO_2 emissions, and to eliminate centralized power system issues, it is crucial to install islanded MG using clean, renewable, and sustainable power plants. Moreover, the optimal size configuration for hybrid power plants is an issue that this study aims to address. The main issue is selecting the optimal capacity to reduce system costs while maximizing reliability. However, optimum sizing techniques cannot be carried out until the components to be hybridized have been mathematically modeled.

Table 2. Fuel and operation costs of conventional power plants.

Cost ($/kWh)	Fuel	Operation
Gas turbines Cost	0.067	0.041
Thermal Cost	0.016	0.009
Diesel Cost	0.016	0.009

3. System Description

Figure 2 represents the structure of the islanded MG to be optimized. This MG consists of AC and DC buses that are linked through a bidirectional main inverter.

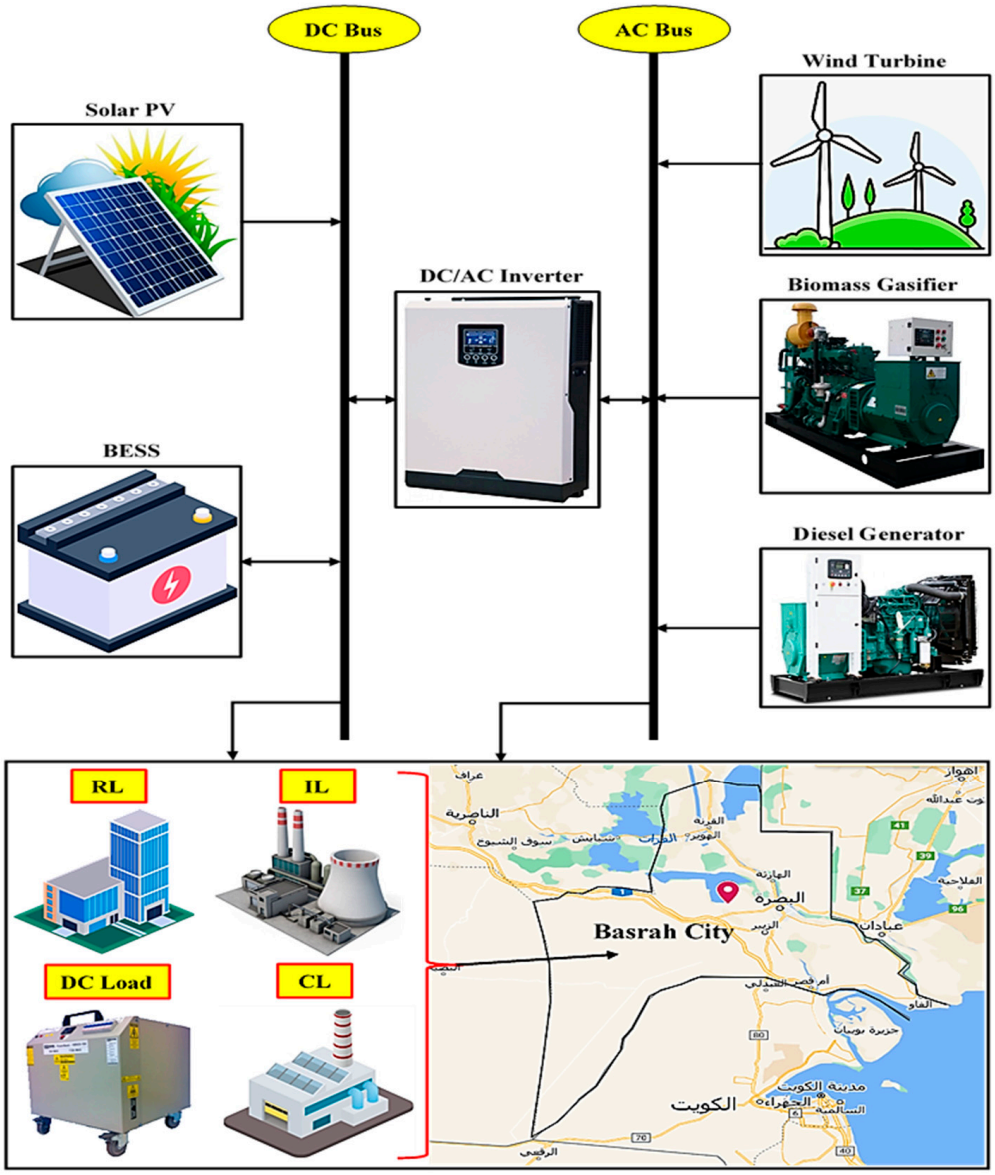

Figure 2. The proposed IMG.

Solar PV, DC loads, and BESS are linked to the DC bus, while wind turbine, diesel generator, and biomass gasifier are connected to the AC bus. The primary purpose of the electricity generation is to meet the load requirement of the Basra city. The size evaluation approach takes into account the system's load profile, reliability restrictions, and economic and environment data. Once the foundation is laid, the assessment approach executes a year-long optimization model simulating an economic dispatch with the goal of reducing the annual cost and meeting the load.

3.1. Climatological and Load Data of Basra

As solar and wind energy are only available intermittently, hybrid systems are typically employed to ensure uninterrupted power. Input parameters for program simulations include data such as load demand, component costs, solar irradiance, temperature, and wind speed. The input utilized weather parameters for various components are illustrated in Figure 3. In winter, Basra can receive 965 W/m^2 and in summer, 1040 W/m^2. The wind speed in Basra can reach 10 m/s or more. As mentioned before, Basra is the excellent place for collecting both wind and solar power.

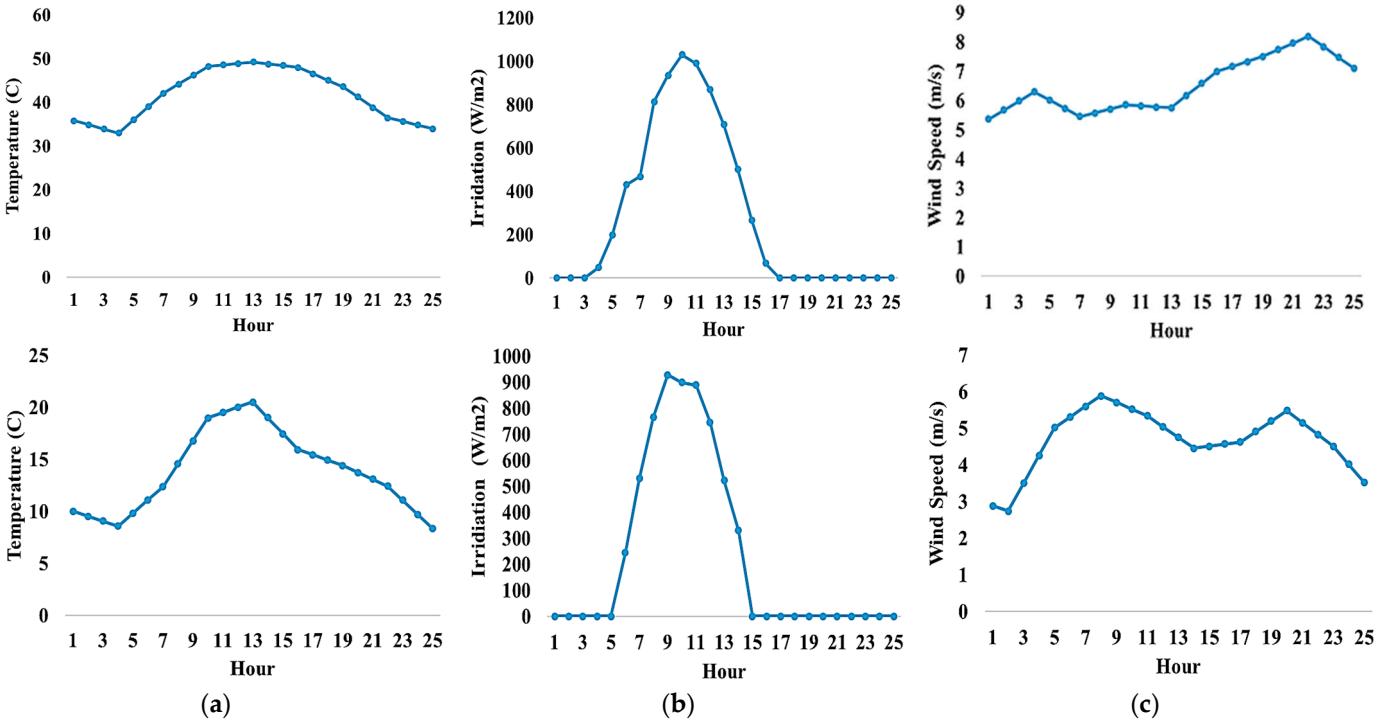

Figure 3. Daily summer (in the top) and winter (in the bottom) weather data for Basra (**a**) solar temperature, (**b**) solar irradiance and (**c**) wind speed.

Electricity consumption may be influenced by several factors, such as the economy, the weather, and how efficiently loads are managed. The annual load profile is shown in Figure 4. Figure 5a shows the daily summer load in Basra for the first day of August, whereas the daily winter load (the first day of December) is depicted in Figure 5b. As seen in Figure 5, the summer loads are greater than the winter loads. The peak season for demand is between June and September, when high summer temperatures necessitate the usage of air conditioning. Consequently, the high electrical demands are driven by variations in the weather, particularly the increase or decrease in temperature and humidity. In the southern Iraqi city of Basra, where summer temperatures and humidity are quite high, consumers do not switch off the air conditioning, and air chillers are ineffective for cooling. It is evident that summertime loads and winter loads differ greatly, and that the summer peak load is larger than the winter peak load.

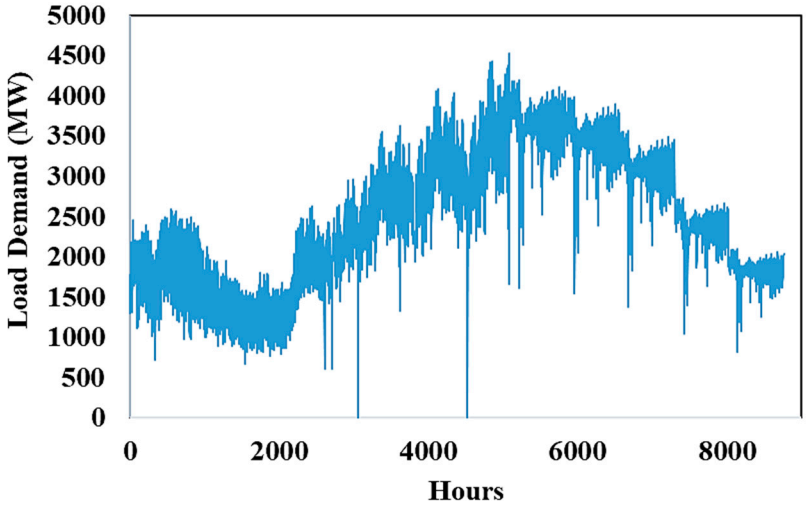

Figure 4. Annualized load data for Basra.

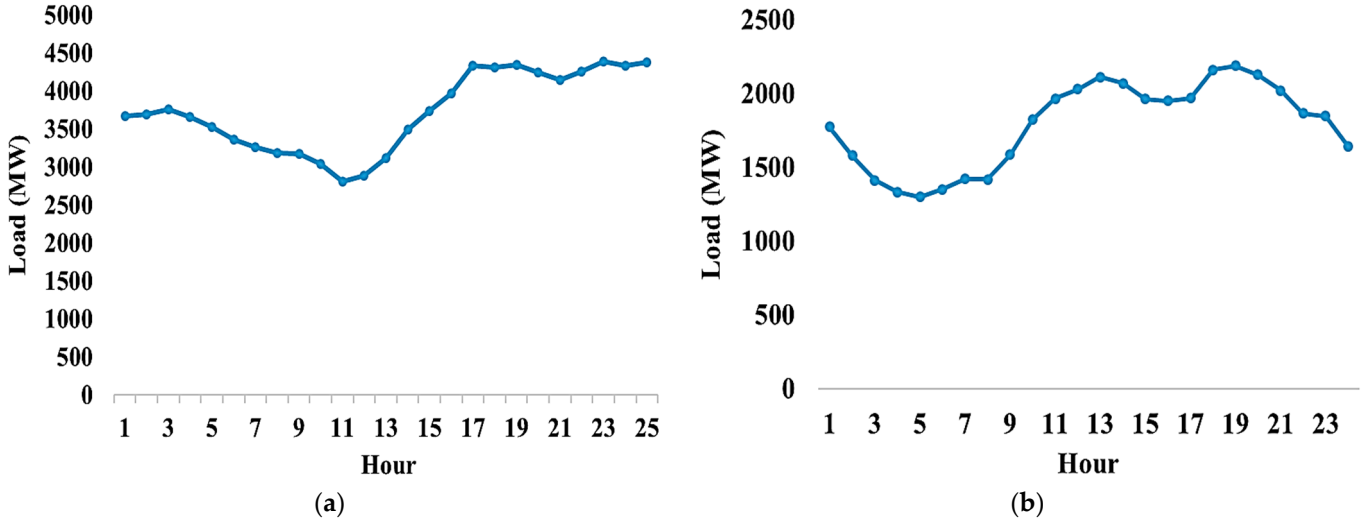

Figure 5. Daily summer and winter loads in Basra for (**a**) the first day of December and (**b**) the first day of August, respectively.

3.2. Dispatch Strategy

The proposed hybrid islanded MG system relies on solar PV, WT, biomass gasifier, battery units, with the diesel generator serving as a backup. First priority is given to renewable solar and wind energies to supply demand, followed by battery units to handle energy shortages. Then, if the available resources are insufficient to fulfill demand, a biogasifier energy source is utilized. Finally, a nonrenewable source (diesel generator) is employed if all adopted energy sources are deficient to meet demand. An optimal hybrid system size can be determined by considering the available RESs, the load at the chosen site, the economic and technical features of the hardware components, and the dispatch technique. The dispatch strategy or energy management algorithm have a significant impact on the optimal size and, as a result, on the post-optimization performance indicators. Since a load-following dispatch approach can reduce wasteful energy consumption and has cheaper LCOE and annual cost values, it is the focus of this research. Figure 6 shows the proposed operational energy management strategy. Figure 7 shows a pseudocode-based proposed energy management strategy.

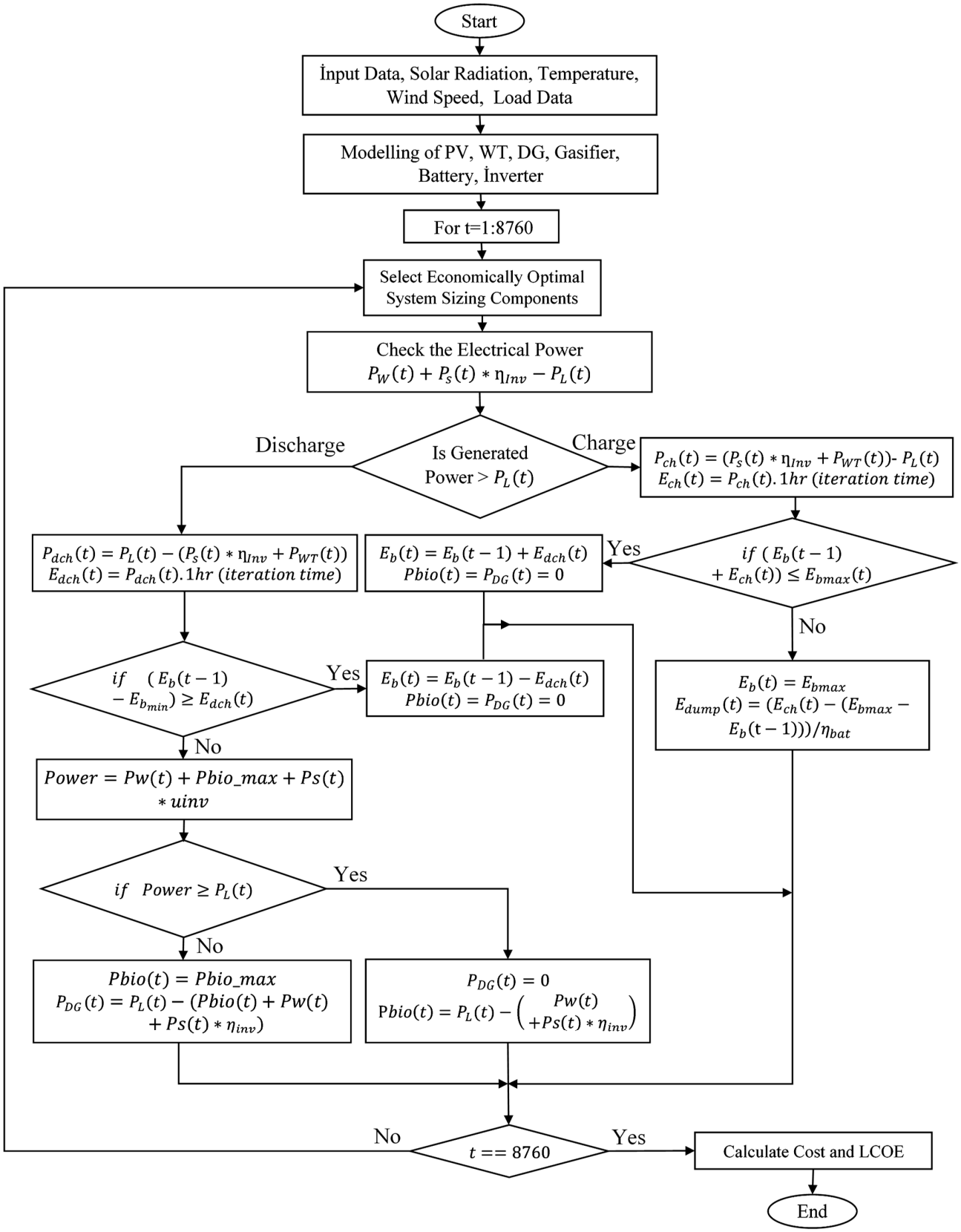

Figure 6. The proposed optimal sizing-based operational energy management strategy.

Abbreviation adopted in Pseudo-code:

$Pw(t)$ = Wind power, $Ps(t)$= Solar power, $P_{bio}(t)$ = Gasifier power, $Pbio_{max}$= Gasifier rated power, $PL(t)$ =Load demand at time t, $P_{ch}(t)$ = Power available for battery charging, $E_{ch}(t)$ =Energy charged to the battery, $E_{dump}(t)$ =Energy that can be used for deferrable load, $P_{dch}(t)$= Power that is to be discharged from battery, $E_{dch}(t)$ =Energy discharged from battery, $E_{b_{max}}$= Maximum battery energy, $E_b(t)$= Energy of the battery at time t, $P_{DG}(t)$= energy produced by DG at time t, $DG_{hr}(t)$=1 DG is started at time t, η_{Inv} =inverter efficiency, η_{bat} =battery efficiency.

Pseudo-code of Energy Management Strategy:

***Input data**: solar radiation, temperature, wind speed, and load data.*

$n \leftarrow 8760$

for $t \leftarrow 1, n$ ***do***

Apply Eqns. (1, 2, 4, 7, and 10) to generate power of each power resource.

$P_{ch}(t) \leftarrow (Pw(t) + Ps(t) * \eta_{Inv}) - PL(t)$

$E_{ch}(t) \leftarrow P_{ch}(t).1hr\ (iteration\ time)$

if $E_{ch}(t) \leq E_{b_{max}} - E_b(t-1)$ ***do***

$E_b(t) \leftarrow E_b(t-1) + E_{ch}(t)$

end if

else if

$E_b(t) \leftarrow E_{b_{max}}$

$E_{dump}(t) \leftarrow \left(E_{ch}(t) - \left(E_{b_{max}} - E_b(t-1)\right)\right)/\eta_{bat}$

$E_{ch}(t) \leftarrow E_{b_{max}} - E_b(t-1)$

end if

$P_{dch}(t) \leftarrow PL(t) - (Pw(t) + Ps(t) * \eta_{Inv})$

if $P_{dch}(t) \geq PL(t)$ ***do***

if $(E_b(t-1) - E_{b_{min}}) \geq E_{dch}(t)$ ***do***

$E_b(t) \leftarrow E_b(t-1) - E_{dch}(t)$

end if

end if

if $PL(t) \leq (Pw(t) + Pbio_{max} + Ps(t) * \eta_{Inv})$ ***do***

$Pbio(t) \leftarrow PL(t) - (Pw(t) + Ps(t) * \eta_{Inv})$

else if

$P_{DG}(t) \leftarrow P_L(t) - (Pbio(t) + Pw(t) + Ps(t) * \eta_{inv})$

$Pbio(t) \leftarrow Pbio_{max}$

$DG_{hr(t)} \leftarrow 1$

end if

end if

end for

Figure 7. A proposed pseudocode-based energy management strategy.

4. Mathematical Modeling of the Proposed System

4.1. Solar PV

According to [54,55], Equation (1) combines all the essential elements that determine PV output, such as solar radiation and temperature. A solar PV panel's power output can be written as

$$P_s(t) = \frac{G \times P_{PV}^{nom}}{G_{ref}} \left[1 + K\left(T_{amb} + 0.0256 \times G - T_{ref}\right)\right] \tag{1}$$

where $P_s(t)$ represents solar PV output power, PV nominal power under normal test conditions is denoted by P_{PV}^{nom}, solar radiation is denoted by G, reference radiation is denoted by G_{ref} = 1 kW/m^2, and K is the power–temperatures coefficient (for monocrystalline and polycrystalline (Si) solar cells, it is $-3.7 \times 10^{-3}\ 1/C^o$ [56,57]), T_{ref} = 25 °C is the standard temperature at standard conditions, and T_{amb} refers to the ambient temperature.

4.2. Wind Turbine

A wind turbine's output can be determined using the following formula:

$$P_W(t) = \begin{cases} 0 & V(t) \le V_{cin} \text{ and } V(t) \ge V_{cout} \\ P_r^W & V_{rat} \le V(t) \le V_{cout} \\ P_r^W \times \frac{V(t) - V_{cin}}{V_{rat} - V_{cin}} & V_{cin} \le V(t) \le V_{rat} \end{cases} \tag{2}$$

where $P_W(t)$ represents wind turbine output power, P_r^W is the single wind turbine rating power, V_{cin} is the cut-in speed, V_{rat} is the rated wind speed, V_{cout} is the cut-out speed, and $V(t)$ is the required reference height-based wind speed. Hub height wind speeds are not always the same as reference height speeds because they are dependent on both the geographical location and the site. The full form of this expression is as follows:

$$V(t) = V_r(t) \times \left(\frac{H_{WT}}{H_r}\right)^{\lambda} \tag{3}$$

where $V(t)$ denotes the wind speed at height H_{WT}, $V_r(t)$ denotes the wind speed at the reference height (H_r), and is the friction coefficient. For flat, well-lit areas, the friction coefficient is often just 1/7, according to studies [58,59].

4.3. Battery Unit

When PV and WT renewable energies are insufficient, a hybrid system can use batteries to store extra energy and release it when needed. An accurate estimate of the charge state allows for the measurement of energy. Using the following formula, one may determine the SOC of a battery as a function of time [58,59].

$$\frac{SOC(t)}{SOC(t-1)} = \int_{T-1}^{T} \frac{P_b(t) \times \sqrt{\eta_{batt}^c \eta_{batt}^d}}{V_{bus}} dt = \int_{T-1}^{T} \frac{P_b(t) \times \eta_{batt}}{V_{bus}} dt \tag{4}$$

where V_{bus} represents the bus voltage, $P_b(t)$ the input/output power, and η_{batt} denotes the round trip efficiency of the battery. Positive $P_b(t)$ indicates that the battery is being charged; negative $P_b(t)$ indicates that the battery is being discharged. The battery's charging efficiency is denoted by η_{batt}^c, and its discharging efficiency is denoted by η_{batt}^d [60].

The efficiency of charging is assumed to be 85%, while the efficiency of discharging is assumed to be 100%. The aggregate capacity (C_n) of a battery bank is equivalent to the maximum state of charge (SOC_{max}). This idea is stated as follows:

$$C_n(Ah) = \frac{N_{batt} \times V_{batt}}{V_{bus}} C_b(Ah) \tag{5}$$

where C_b is the battery capacity, N_{batt} is the number of batteries, and V_{batt} represents the battery voltage. There is a minimum state of charge, denoted by SOC_{min}, which the battery bank must not be discharged. If the battery bank is being heavily utilized, this restriction can serve as a system constraint. The required bus voltage is attained by connecting batteries in series.

Maximum charge and discharge power are also important factors to consider when simulating battery behavior. It is determined by the following formula and is directly proportionate to the maximum charge current.

$$P_b^{max} = \frac{N_{batt} \times I_{max} \times V_{batt}}{1000} \tag{6}$$

where I_{max} represents the maximum charge current.

4.4. Diesel Generator Modeling

The diesel generator is utilized as a backup power supply if the renewable energy sources and battery bank are insufficient to meet the required load power demand. The diesel generator's hourly fuel consumption can be determined using the following equation [61,62]:

$$F(DG) = A \times P_{DG}(t) + B \times P_{DG}^{rated} \tag{7}$$

where $F(DG)$ is the generator's fuel consumption in liters per hour, $P_{DG}(t)$ is the output power in kilowatts, P_{DG}^{rated} is the generator's rated output in kilowatts, A is the slope coefficient of the fuel curve, and B is the intercept coefficient. The values of A and B employed in this investigation are 0.2461 L per hour per output kilowatts and 0.08415 L per hour per rated kilowatts [61,62].

To calculate the cost of fuel consumption, one can use the following formula [63]:

$$FCC_{DG} = FC_{DG} \times F(DG) \tag{8}$$

where FCC_{DG} is the cost of fuel consumption, and FC_{DG} represents the fuel cost per liter, which is assumed to be USD 0.3/liter.

4.5. Biomass Gasifier

Through a process called biomass gasification, solid bio-residue is transformed into a gaseous fuel that can be burned to power generators. In the case of a biomass gasifier, the producer gas generated during partial combustion serves as an input fuel. A biomass gasifier's yearly electricity output in kilowatt-hours can be determined by using the formula

$$E_{bio} = P_{bio} \times 365 \times CUF \times Operating\ Hours/Day \tag{9}$$

where E_{bio} represents the biomass gasifier's yearly electricity output, CUF represents the capacity utilization factor and P_{bio} represents the system's rating power. Several factors, including the biomass's calorific value, its availability (Ton/year), and the biomass gasifier's operating hours, are crucial in a biomass-based energy system. The following is the maximum capacity for a biomass gasifier:

$$P_{bmg}^{m} = 1000 \times Total\ biomass\ avialable \left(\frac{Ton}{yr}\right) \times CV_{bm} \times \eta_{bmg} \tag{10}$$

where P_{bmg}^{m} denotes the maximum capacity for a biomass gasifier, CV_{bm} represents the calorific value of the biomass and η_{bmg} represents the overall efficiency of converting biomass to electricity [58,59].

4.6. Power Converter Modeling

Having both DC and AC buses necessitates the use of a power DC/AC converter. The peak power demand establishes the size of the converter. As shown in Equation (11), the inverter power rating can be calculated [59].

$$P_{inv}(t) = \frac{P_L^{max}(t)}{\eta_{inv}} \tag{11}$$

where $P_{inv}(t)$ represents the inverter power rating, η_{inv} represents the inverter's efficiency, and $P_L^{max}(t)$ is the peak power demand.

5. Optimization Technique

Using a combination of algorithms to find better solutions for optimization problems has become increasingly popular in recent years. Hybrid optimized algorithms are more effective at resolving the problems because they incorporate many well-known optimization techniques. The GWO algorithm models the hunting process and pack structure of gray wolves. There are four different kinds of wolves represented here. The alpha (α) wolf is the pack's dominant member and occupies the pinnacle of the social hierarchy.

There is no requirement that the alpha be the strongest wolf in the pack, but it does have to be the best leader. It is responsible for coordinating the group's activities, such as foraging and predation. The alpha assistant beta (β), who is situated on the second level of the pyramid and assists the alpha in leading the group. Delta (δ), the third-level wolf, must obey the commands of the upper wolves, alpha and beta. When an alpha or beta has reached the end of its useful life, it is demoted to delta. The letter omega (ω) denotes the bottom of the pyramid. Omega is obligated to follow the group's directives [59].

The meta-heuristic algorithms GWO and cuckoo search (CS) are widely used today. However, their methods of searching are different. The CS algorithm is inspired by cuckoos' parasitic breeding. Cuckoo parasitism on other birds' broods serves as inspiration for CS, which employs Lévy flight to come up with original ideas. Many studies have shown that GWO is more adept at exploitation, while CS is more drawn to global exploration [59]. The optimal sizes of the suggested system components have been determined using the GWO algorithm, which reduces the system's cost while still satisfying the load demand. Inspecting a high-fitness individual with GWO causes a reduction in global search ability, making it easier to settle for a suboptimal solution. When it comes to updating the nest's position, a CS Algorithm (CSA) does so with a probability that fluctuates and is not tied to the search path. This makes traveling between different spaces of the world a lot less difficult. Therefore, CSA is a powerful method that can be implemented to enhance GWO.

5.1. Mathematical Model of GWO

The level of grey is governed by the fitness function. It turns out that the alpha wolf, the beta wolf, and the delta wolf are the top three fitness options. The key-group designates these three solutions. The alpha wolf is responsible for the pack's welfare. In order to develop GWO, researchers have mathematically modeled the social structure and hunting strategies of grey wolves. The following are the proposed mathematical models for social hierarchy, encircling, hunting, and attacking prey [64,65]:

1. Encircling prey

Grey wolves often use a pack strategy to catch prey. For a mathematical description of encircling behavior, we provide the following equations:

$$\vec{D} = \left| \vec{X_p}(t) \times \vec{C} - \vec{X}(t) \right| \tag{12}$$

$$\vec{X}(t+1) = \left| \vec{X_p}(t) - \vec{A} \times \vec{D} \right| \tag{13}$$

where the position of a single wolf is denoted by $\vec{X}$, and $t+1$ represents the next iteration. The vectors A and D are the coefficients, and the vector ($\vec{X_p}$) denotes the position of the prey. The process of calculation is represented by the following equations.

$$\vec{A} = 2 \times a \times r_1 - a \tag{14}$$

$$\vec{C} = 2 \times r_2 \tag{15}$$

where r_1 and r_2 are two arbitrary positive integers between zero and one. To achieve a linear decrease in the number of iterations, the vector a is given a value between 2 and 0.

2. Hunting prey

When the pack locates prey, the alpha, beta, and delta wolves are responsible for encircling it. It is safe to assume they have already spotted the prey. Consequently, a key-group is formed by combining the top three solutions and reordering the wolves accordingly. The position is updated using the following equations.

$$\vec{X}(t+1) = \frac{\vec{X}_x + \vec{X}_y + \vec{X}_z}{3} \tag{16}$$

$$\vec{X}_x = \left| \vec{X}_\alpha - \vec{A}_1 \times \vec{D}_\alpha \right| \tag{17}$$

$$\vec{X}_y = \left| \vec{X}_\beta - \vec{A}_2 \times \vec{D}_\beta \right| \tag{18}$$

$$\vec{X}_z = \left| \vec{X}_\delta - \vec{A}_3 \times \vec{D}_\delta \right| \tag{19}$$

where $\vec{X}_\alpha$, $\vec{X}_\beta$, and $\vec{X}_\delta$ represent the best three solutions so far in the iteration process, which together form the key-group. More parameters are defined by the following equations.

$$\vec{D}_\alpha = \left| \vec{C}_1 \times \vec{X}_\alpha - \vec{X} \right| \tag{20}$$

$$\vec{D}_\beta = \left| \vec{C}_2 \times \vec{X}_\beta - \vec{X} \right| \tag{21}$$

$$\vec{D}_\delta = \left| \vec{C}_3 \times \vec{X}_\delta - \vec{X} \right| \tag{22}$$

3. Attacking prey

For grey wolves, the moment an animal stops moving is the perfect time to pounce. As a result, the following formula describes how grey wolves approach their prey.

$$a = 2 - \frac{2 \times t}{Max} \tag{23}$$

where t is an integer between zero and the maximum number of iterations of the current algorithm (max iteration number).

5.2. Cuckoo Search

One popular meta-heuristics algorithm takes inspiration from cuckoos' parasitic breeding behavior and is known as cuckoo search (CS) [62]. An analogy of the cuckoo egg in computer science is the solution. The CS algorithm should follow the three guidelines presented. Firstly, cuckoo birds lay only one egg at a time and choose their nests at random. Second, only the best nests will produce offspring that are desirable. Third, there is a

predetermined number of bird nests and an equal chance of finding an egg. The host bird will leave the nest if it finds an intruder's egg and start a new one. During iteration, the nests are kept up-to-date by applying the next equations in accordance with the aforementioned three rules. At each iteration, a new set of candidate solution, $X_i^t (i \in [1, \ldots, N])$ is generated using Lévy flight by introducing a shift of position c_i into the current value of X_i^t. To find c_i, a random step, s_i, is generated by a symmetric Levy distribution. Utilizing Mantegna's algorithm to generate s_i [59,66]:

$$s_i = \frac{\vec{u}}{\left|\vec{v}\right|^{1/\beta}} \tag{24}$$

where the random numbers u and v are, respectively, satisfied by the normal distribution [62]:

$$u \sim N\left(0, \sigma_u^2\right), \quad v \sim N\left(0, \sigma_v^2\right) \tag{25}$$

$$\sigma_u = \frac{\Gamma(1+\beta) \times \sin\left(\frac{\beta\pi}{2}\right)}{\Gamma\left(\frac{(1+\beta)}{2}\right) \times \beta \times 2^{(\beta-1)/2}}, \ \sigma_v = 1 \tag{26}$$

where gamma $\Gamma(.)$ stands for the gamma function.

Following the determination of s_i, the necessary shift in coordinates c_i is determined as follows.

$$c_i = 0.01 \times s_i \oplus \left(X_i^t - X^{best}\right) \tag{27}$$

where $\oplus$ is an entry-wise multiplication and X^{best} is the best solution found so far in terms of fitness. Finally, we use Equation (28) to find the new candidate solution, X_i^{t+1}.

$$X_i^{t+1} = X_i^t + c_i \tag{28}$$

5.3. Hybridized Grey Wolf and Cuckoo Search

Formula (16) demonstrates that the GWO algorithm uses a key-group called trend search to update the positions of high-fitness individuals. Therefore, it will be unable to perform well in global searches and may easily settle for a suboptimal solution when working with large sets of data. The CS algorithm repositions the nest using a random walk and levy-flights, where the length of the search path and the direction of travel are both highly arbitrary. As a consequence of this, the CS algorithm is able to seek the solution space effectively due to the fact that its step changes with the detection of small distances and occasionally walks over long distances, and the step length becomes significantly longer over the course of the algorithm. The pseudocodes for the GWO and GWCSO algorithms are shown in Figure 8.

In this work, CSA is used within the GWO algorithm to both refine the locations of previously established search agents and generate a brand new group. By obtaining the sizing components of solar PV, wind turbine, storage batteries, and biomass gasifier in an islanded MG, the new hybrid GWCSO is effective and can solve optimization problems rapidly. Here, the grey wolf agent's position, velocity, and convergence accuracy are adjusted using the CS position updated equation. Equation (28) has been used to update Equations (16)–(19).

Algorithm 1: Pseudo-code of GWO

Initialize grey wolf population X_i ,$i = \overline{1,n}$, *a, A, and C*
$X_\alpha \leftarrow$ *best search agent*
$X_\beta \leftarrow$ *second best search agent*
$X_\delta \leftarrow$ *third best search agent*
while $t < t_{max}$ ***do***
    for *each search agent* $\in X_i$ ***do***
    Calculate $\vec{X}_x$, $\vec{X}_y$, $\vec{X}_z$ *using eqns. (17-19)*
    $\vec{X}(t) \leftarrow \frac{\vec{X}_x+\vec{X}_y+\vec{X}_z}{3}$
    end for
$r_1 \leftarrow rand()$
$r_2 \leftarrow rand()$
$a \leftarrow 2 - (2 \times t)/t_{max}$
$\vec{A} \leftarrow 2 \times a \times r_1 - a$
$\vec{C} \leftarrow 2 \times r_2$
Calculate the fitness of all search agents
Update X_i
$t \leftarrow t+1$
end while
Return X_α

(**a**)

Algorithm 2: Pseudo-code of GWCSO

Initialize grey wolf population X_i ,$i = \overline{1,n}$, *a, A, and C*
$X_\alpha \leftarrow$ *best search agent*
$X_\beta \leftarrow$ *second best search agent*
$X_\delta \leftarrow$ *third best search agent*
while $t < t_{max}$ ***do***
    for *each search agent* $\in X_i$ ***do***
    Calculate $\vec{X}_x$, $\vec{X}_y$, $\vec{X}_z$ *using eqns. (17-19)*
    $\vec{X}(t) \leftarrow \frac{\vec{X}_x+\vec{X}_y+\vec{X}_z}{3}$
    end for
$r_1 \leftarrow rand()$
$r_2 \leftarrow rand()$
$a \leftarrow 2 - (2 \times t)/t_{max}$
$\vec{A} \leftarrow 2 \times a \times r_1 - a$
$\vec{C} \leftarrow 2 \times r_2$
Calculate the fitness of all search agents
Update X_i
$c_i \leftarrow 0.01 \times s_i \oplus (X_i^t - X^{best})$
$X_i(t) \leftarrow X_i^t + c_i$
$t \leftarrow t+1$
end while
Return X_α

(**b**)

Figure 8. The pseudocode of (**a**) GWO and (**b**) GWCSO.

6. Objective Functions and Economic Modeling

This paper optimizes the energy flow-based component sizing of the hybrid energy system while reducing the total annualized cost (ANC). The number of WT, solar PV panels, battery capacity, and biomass gasifier rating have been selected as the four major decision factors for optimal configuration. The concepts of ANC and $LCOE$ are utilized in this economic analysis. The solution with the smallest values of all constraints and parameters is proven to be the best solution. The replacement cost, operational and maintenance cost, salvage cost, and total capital cost make up the objective function of the overall system cost. The main objective function that needs to be minimized within the given constraints is taken to be the following function: Minimizing ANC

$$ANC = F\left(N_s C_s + N_W C_W + N_{bat} C_{bat} + P_{inv} C_{inv} + P_{bmg} C_{bmg} + P_{DG} C_{DG}\right) \quad (29)$$

where C_W, C_s, C_{inv}, and C_{bat} represent the cost of a wind turbine (per kilowatt-hour), solar PV panel (per kilowatt-hour), inverter (per kilowatt-hour), and battery (per unit), respectively. C_{bmg} represents the biomass gasifier's price (per kilowatt) and P_{bmg} represents its power output. C_{DG} denotes the diesel generator's cost (per kilowatt) and P_{DG} represents its

power output. The inverter has a power output of P_{inv}. The total number of wind turbines, solar photovoltaic panels, and batteries are denoted by N_W, N_s, and N_{bat}, respectively.

The ANC of an installed component includes the capital costs, replacement costs, salvage costs, annual operation and maintenance costs. Additionally, the total ANC value can be expressed as follows for each component:

$$C_s = C_s^c + C_s^r + C_s^{om} - C_s^s \tag{30}$$

$$C_w = C_w^c + C_w^r + C_w^{om} - C_w^s \tag{31}$$

$$C_{batt} = C_{batt}^c + C_{batt}^r + C_{batt}^{om} - C_{batt}^s \tag{32}$$

$$C_{inv} = C_{inv}^{ci} + C_{inv}^r + C_{inv}^m - C_{inv}^s \tag{33}$$

$$C_{bmg} = C_{bmg}^{ci} + C_{bmg}^r + C_{bmg}^m - C_{bmg}^s \tag{34}$$

$$C_{DG} = C_{DG}^{ci} + C_{DG}^r + C_{DG}^m - C_{DG}^s \tag{35}$$

where the capital costs denoted by C^c, C^r represents the replacement costs, and C^s represents the salvage costs, annual operation and maintenance costs denoted by C^{om}.

The objective function is minimized while a number of constraints are enforced, which can be summed up as follows:

$$1 \leq N_s \leq N_s^{max} \tag{36}$$

$$1 \leq N_W \leq N_W^{max} \tag{37}$$

$$1 \leq P_{bmg} \leq P_{bmg}^{max} \tag{38}$$

$$1 \leq N_{batt} \leq N_{batt}^{max} \tag{39}$$

$$SOC_{min} \leq SOC \leq SOC_{max} \tag{40}$$

where N_s^{max}, N_{batt}^{max}, *and* N_W^{max} represent the maximum numbers of solar PV panels, batteries, and wind turbines, and P_{bmg}^{max} represents the maximum rating of a biomass gasifier.

$$C_s^T = N_s\left\{C_s^c + \left[C_s^{om} \times \frac{(i)(i+1)^N - 1}{(i)(i+1)^N}\right] - \left[C_s^{sal} \times \frac{PV\ Life - N}{PV\ Life}\right]\right\} \tag{41}$$

$$C_W^T = N_W\left\{C_W^c + \left[C_W^r \times \sum_{Z=1}^{(\frac{N}{WT\ Life}-1)}\left(1 + \frac{1}{(i+1)^{Z\times WT\ Life}}\right)\right] + \left[C_W^{om} \times \frac{(i)(i+1)^N-1}{(i)(i+1)^N}\right] - \left[C_W^{sal} \times \frac{WT\ Life-N}{WT\ Life}\right]\right\} \tag{42}$$

$$C_{batt}^T = N_{batt}\left\{C_{batt}^c + \left[C_{batt}^r \times \sum_{Z=1}^{(\frac{N}{batt\ Life}-1)}\left(1 + \frac{1}{(i+1)^{Z\times batt\ Life}}\right)\right] + \left[C_{batt}^{om} \times \frac{(i)(i+1)^N-1}{(i)(i+1)^N}\right] - \left[C_{batt}^{sal} \times \frac{batt\ Life-N}{batt\ Life}\right]\right\} \tag{43}$$

$$C_{inv}^T = P_{inv}\left\{C_{inv}^c + \left[C_{inv}^r \times \sum_{Z=1}^{(\frac{N}{inv\ Life}-1)}\left(1 + \frac{1}{(i+1)^{Z\times inv\ Life}}\right)\right] + C_{inv}^{om} - \left[C_{inv}^{sal} \times \frac{inv\ Life - N}{inv\ Life}\right]\right\} \tag{44}$$

$$C_{bmg}^T = P_{bmg}\left\{C_{bmg}^c + \left[C_{bmg}^r \times \sum_{Z=1}^{(\frac{N}{bmg\ Life}-1)}\left(1 + \frac{1}{(i+1)^{Z\times bmg\ Life}}\right)\right] - \left[C_{bmg}^{sal} \times \frac{bmg\ Life-N}{bmg\ Life}\right]\right\} + Fuel_{consumption} \times BMG\ Fuel_{cost} + \left[C_{bmg}^{om} \times P_{bmg}^m\right] \tag{45}$$

$$C_{DG}^T = P_{DG}^m\left\{C_{bmg}^c + \left[C_{bmg}^r \times \sum_{Z=1}^{(\frac{N}{DG\ Life}-1)}\left(1 + \frac{1}{(i+1)^{Z\times DG\ Life}}\right)\right] + C_{DG}^{om} - \left[C_{DG}^{sal} \times \frac{DG\ Life-N}{DG\ Life}\right]\right\} + F(DG) \times DG\ Fuel_{cost} \tag{46}$$

where N is the project life, i is the interest rate, and P_{DG}^m is the maximum DG energy production.

$$ANC = \frac{(i)(i+1)^N}{(i+1)^N - 1} \times \left(C_s^T + C_W^T + C_{batt}^T + C_{inv}^T + C_{bmg}^T + C_{DG}^T\right) \tag{47}$$

The LCOE is the average cost per kilowatt-hour of usable energy produced by the system.

$$LCOE = \frac{ANC\left(\frac{\$}{Year}\right)}{Total\ useful\ energy\ served\left(\frac{kWh}{Year}\right)} \quad (48)$$

Table 3 displays all of the economic and technical parameters related to the proposed MG's components [59,67].

A microgrid's "Renewable Factor" (RF) is the ratio of its power generated from renewable sources relative to the power generated from nonrenewable sources [68,69]. When the RF is 100%, the system is considered to be in its ideal state and is wholly powered by renewable energy sources. When it is equal to 0, it means that the amount of energy produced by renewable energy resources and nonrenewable energy sources is equal [36].

$$\mathrm{RF}(\%) = \left(1 - \frac{\sum Renewable\ Power}{\sum Nonrenewable\ Power}\right) \times 100 \quad (49)$$

Table 3. Technical and economic details of the proposed system's components.

No.	Component Name	Parameter	Value
1	Wind turbine	Rated power	1 kW
		Height	50 m
		Meteorological reference height	20 m
		Min. wind speed for power generation	2 m/s
		Cutout speed	40 m/s
		Rated speed	9 m/s
		Capital cost/kW	900$
		Replacement cost/kW	900$
		Operation and maintenance cost/kW	2 $/year
		Life time	20 years
2	Solar PV	Rated power	1 kW
		Capital cost (per kW)	1100$
		O & M cost (per kW)	4 $/year
		Life time	20 years
		Nominal voltage	6 V
3	Battery	Max charging current	18 A
		Minimum and maximum state of charge	30% and 100%
		Round trip efficiency	92%
		Capital cost (per unit battery)	120$
		Replacement cost (per unit)	100$
		O & M cost (per unit)	2 $/year
		Life time	5 year
		Nominal capacity	100 Ah

Table 3. *Cont.*

No.	Component Name	Parameter	Value
4	Biomass Gasifier	Conversion efficiency	21%
		Capital cost (per kW)	400 $/kW
		Replacement cost (per kW)	300 $/kW
		O & M cost (per kW)	0.01$
		Life time	20,000 h
		Fuel Cost	0.2 $/Kg
5	Diesel Generator	Capital cost (per kW)	175 $/kW
		Replacement cost (per kW)	175 $/kW
		O & M cost (per kW)	3$
		Fuel Cost	0.3 $/Liter
5	Inverter	Efficiency	95%
		Inverter cost	180
		Replacement cost	180
		Operation and maintenance cost	3
		Life time	20 years
6	Other	Interest rate (i) and project Life	6% and 20 years

In this paper, the renewable resources adopted weather inputs according to [70].

7. Simulation Results

The adopted annual ambient temperature, solar irradiance, and wind speed as weather data inputs are shown in Figure 9a, b, and c, respectively. The Basra city total consumption load profile is shown in Figures 5 and 6 and is composed of the Commercial Load (CL), Residential Load (RL), Industrial Load (IL), and DC load. The weather and load data have been adopted in order to identify the optimal size of components and to carry out energy management analysis.

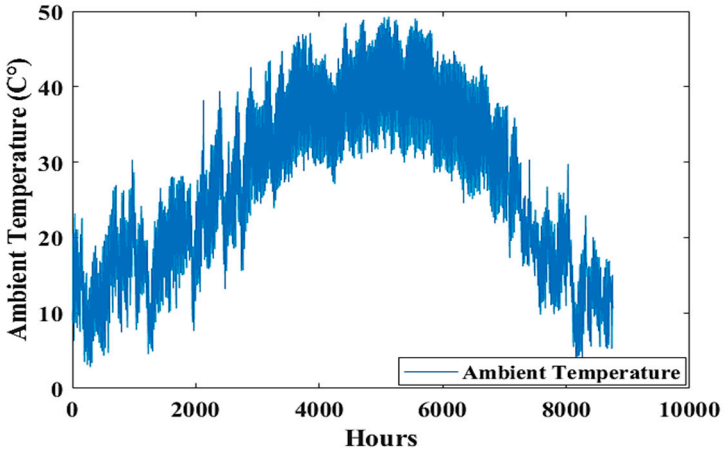

(**a**)

Figure 9. *Cont.*

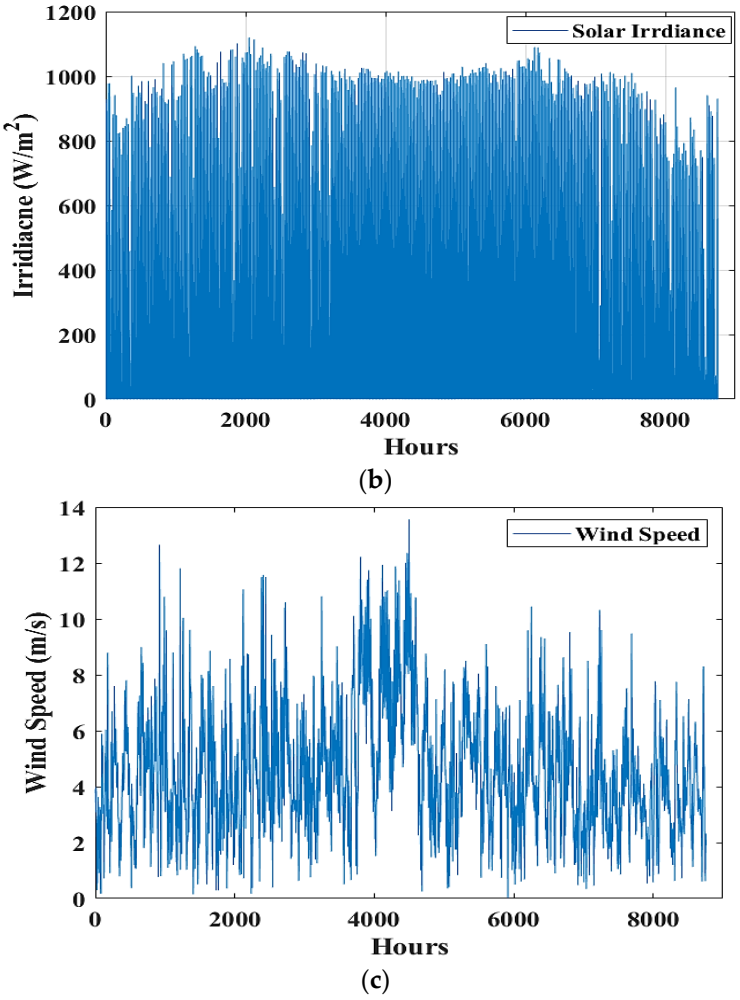

Figure 9. Annualized weather data for Basra (**a**) solar temperature, (**b**) solar irradiance and (**c**) wind speed.

7.1. Optimal Sizing Results

The optimal results include the total required number of WT units, solar PV panels, batteries, and the maximum gasifier rating. Figure 10 illustrates the economic evaluation procedure for determining the optimal configuration. The minimum ANC and LCOE metrics are used to determine which solution is the most cost-effective and practical choice. The optimization algorithms used to model the proposed method in MATLAB are controlled by the parameters shown in Table 4. Figure 11 shows the complete optimal results found by all applied algorithms. The optimal estimated costs for each individual system component are shown in Figure 12. All algorithm-based optimal sizes give nearly identical results. The GWCSO algorithm is able to provide the most optimal solution at the lowest possible cost. The GWCSO estimates 8,683,501.427 kW of solar PV, 1,999,999.046 kW of wind turbines, 26,675,783.63 batteries, and a 3,783,107.662 kW biomass gasifier. Using GWCSO-based proposed MG, the ANC and LCOE metrics are shown in Figure 13a and b, respectively. The GWCSO offers the lowest ANC and LCOE, which are, respectively, 2.6918×10^9 and 0.1192. The solar PV, WT, and biogasifier fractions are shown in Figure 14. The figure clearly shows that 63%, 26%, and 11%, respectively, of the system's total energy production are made up of solar, wind, and bio-gasifier energy. In Figure 15, the adopted algorithms' convergence curves are shown. In light of the findings, it is evident that GWCSO coverage extends down to the ANC's minimum value of 2.6918×10^9, followed by PSO and ALO (2.6919×10^9 and 2.6923×10^9, respectively).

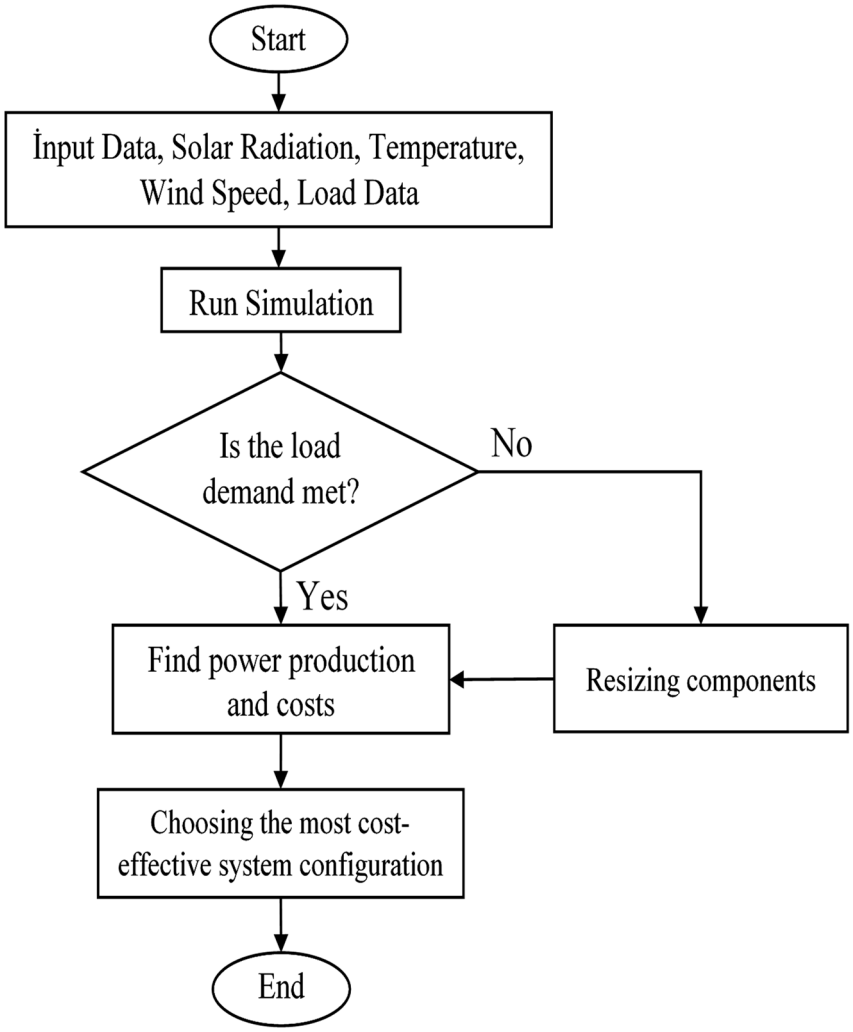

Figure 10. Evaluation flowchart for hybrid system.

Table 4. The control parameters of the adopted algorithms.

Algorithm	Search Agents	Maximum Iterations	Dim	Lower Limits for Wind, Solar, Gasifier and Battery Units	Upper Limits for Wind, Solar, Gasifier and Battery Units	Other
GA	30	300	4	[1 1 1 1]	[2,000,000 15,000,000 5,000,000 100,000,000]	Crossover Probability = 0.8 Mutation Probability = 0.2
PSO	30	300	4	[1 1 1 1]	[2,000,000 15,000,000 5,000,000 100,000,000]	-
CS	30	300	4	[1 1 1 1]	[2,000,000 15,000,000 5,000,000 100,000,000]	-
ALO	30	300	4	[1 1 1 1]	[2,000,000 15,000,000 5,000,000 100,000,000]	-
GWO	30	300	4	[1 1 1 1]	[2,000,000 15,000,000 5,000,000 100,000,000]	-
GWCSO	30	300	4	[1 1 1 1]	[2,000,000 15,000,000 5,000,000 100,000,000]	-

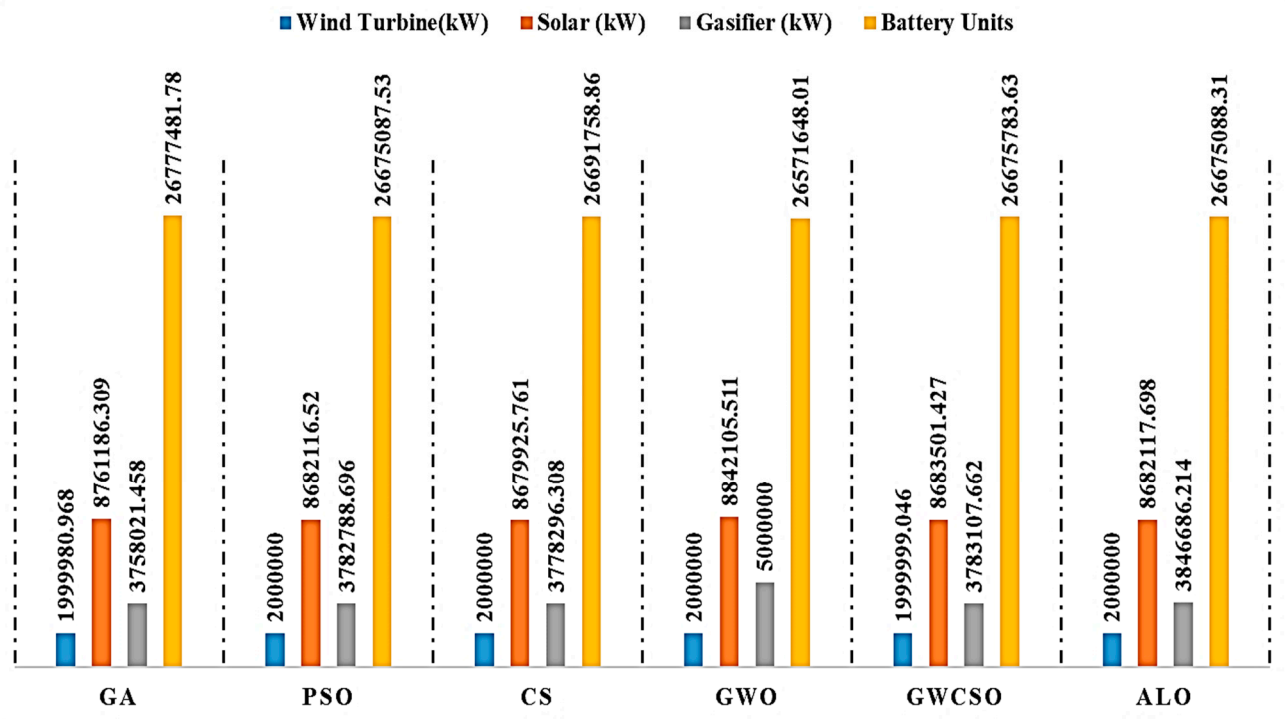

Figure 11. Comprehensively optimal outcomes achieved through the adoption of algorithms.

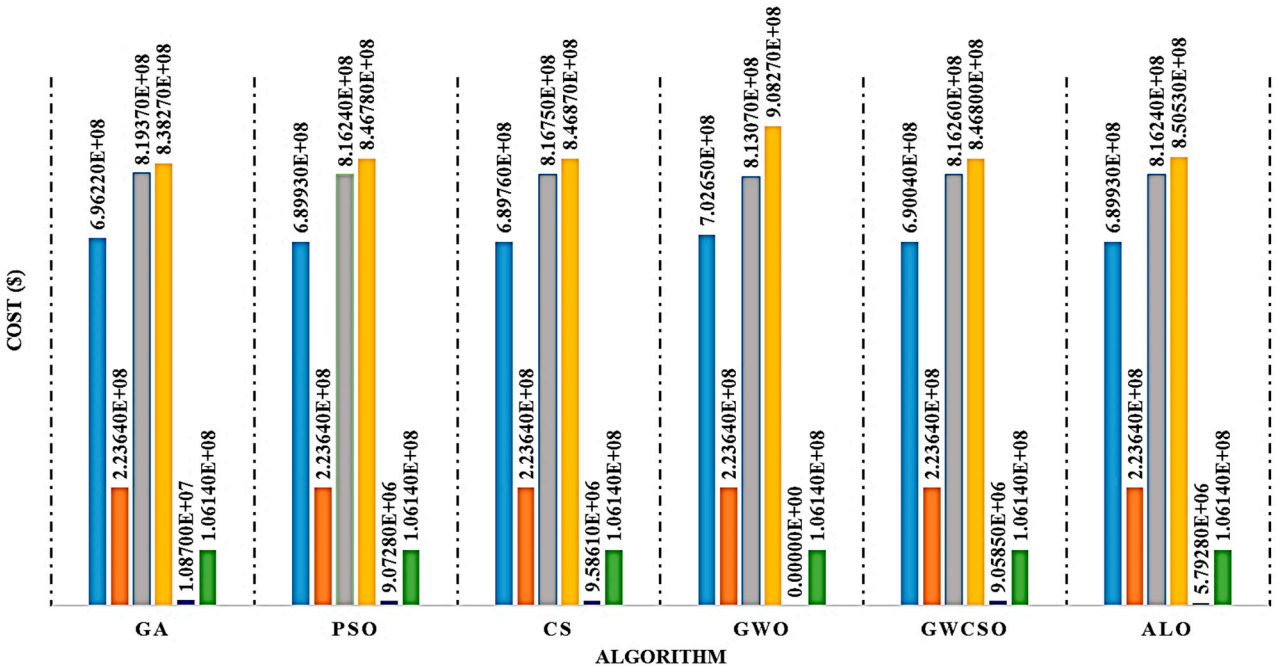

Figure 12. Comprehensively optimal costs of system's components.

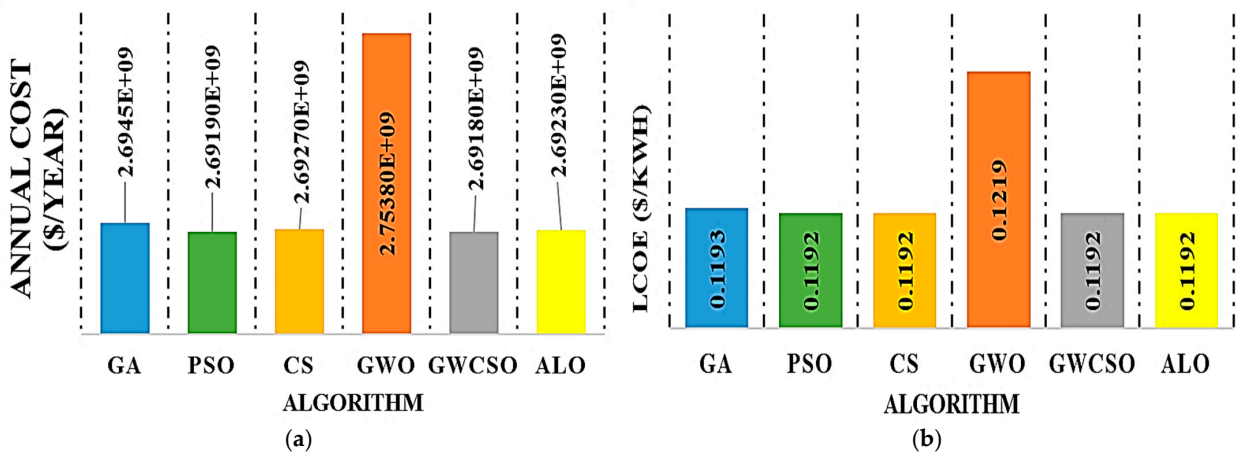

Figure 13. (**a**) ANC and (**b**) LCOE achieved through the adoption of algorithms.

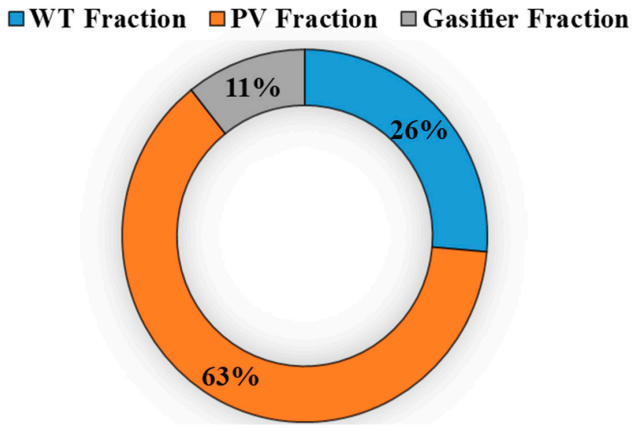

Figure 14. The solar PV, WT, and biogasifier fractions.

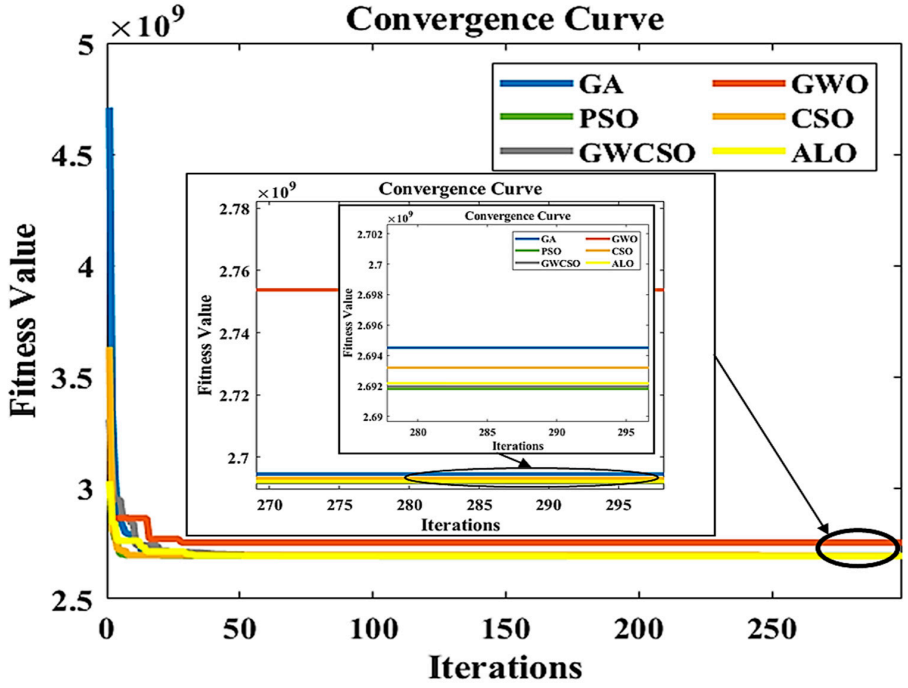

Figure 15. The applied algorithms' convergence curves.

7.2. Energy Management Results

Figure 16a–d, respectively, display the annualized power produced by solar PV, WT, bio-gasifiers, and diesel generators. Similarly, monitoring the charging and discharging rates of the battery is essential, and Figure 17 illustrates the annual input and output energy of the adopted battery units. The excess energy at any one-hour can be utilized as a deferred load or dumped if it is not needed immediately. If the amount of energy needed to discharge exceeds the rate at which batteries can be discharged, a biomass gasifier will be adopted as the power source.

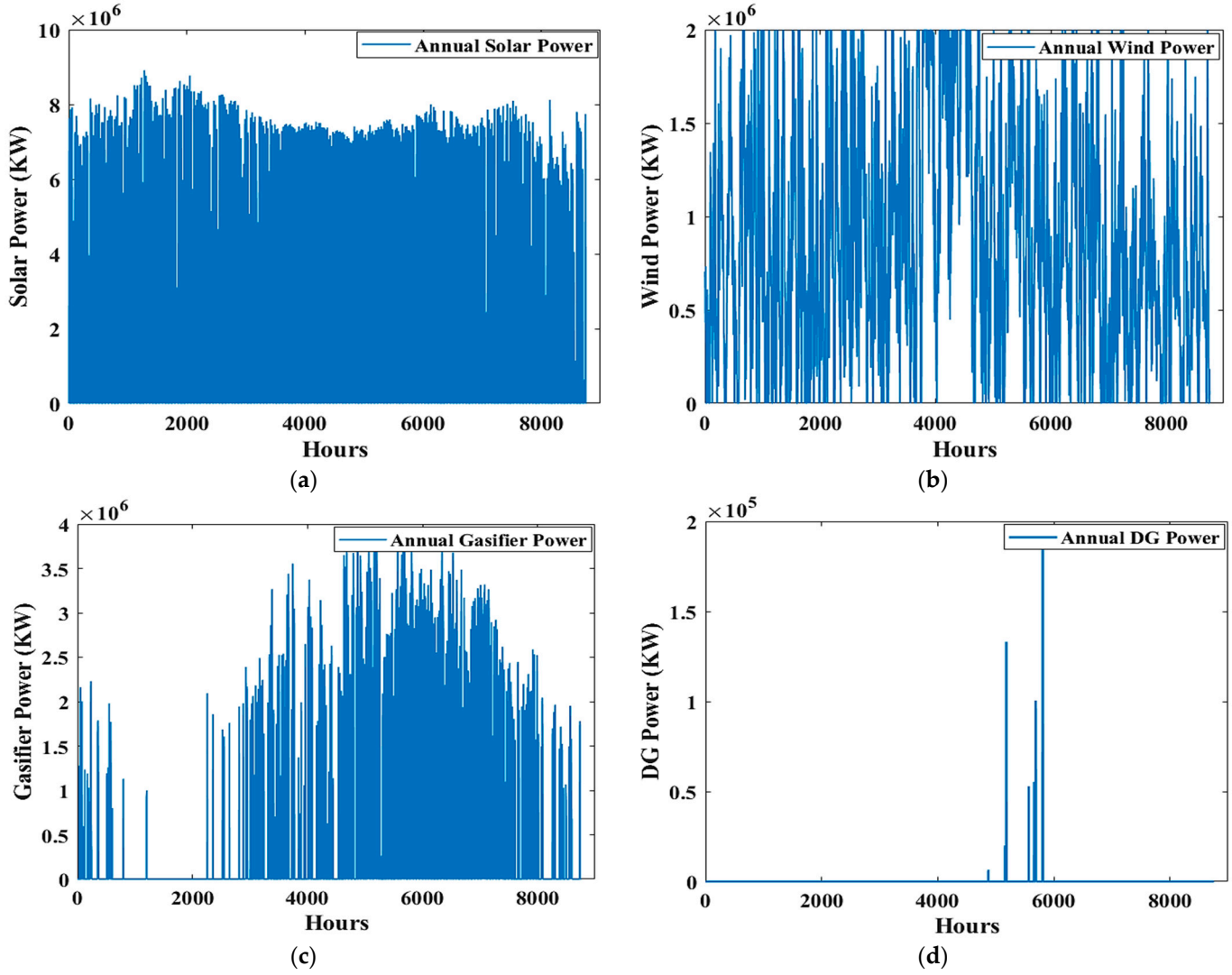

Figure 16. Annual power of (**a**) solar PV, (**b**) wind turbine, (**c**) bio-gasifier, and (**d**) diesel generator.

The proposed system utilized renewable energy sources such as solar panels, wind turbines, batteries, and a gasifier, in addition to the diesel energy as a backup source. The average monthly energy balance over one year is shown in Figure 18. Each monthly bar represents a month's value of energy production from a given source, such as wind, solar PV, batteries (input and output), a gasifier, and a diesel generator. Batteries are used to make up for the shortfall in supply when renewable energy sources cannot meet demand by themselves. The gasifier will provide output power if and only if the combined power from the solar system, the wind, and the batteries output is not sufficient to fulfill the load demand. Therefore, if there is still energy after meeting the load demand, it is essential to determine whether it can all be stored in the battery; if so, the residual energy must be

stored in the battery. When solar PV, WT, batteries, and the bio-gasifier are unable to supply enough energy to meet demand, a diesel generator is used to make up the shortfall.

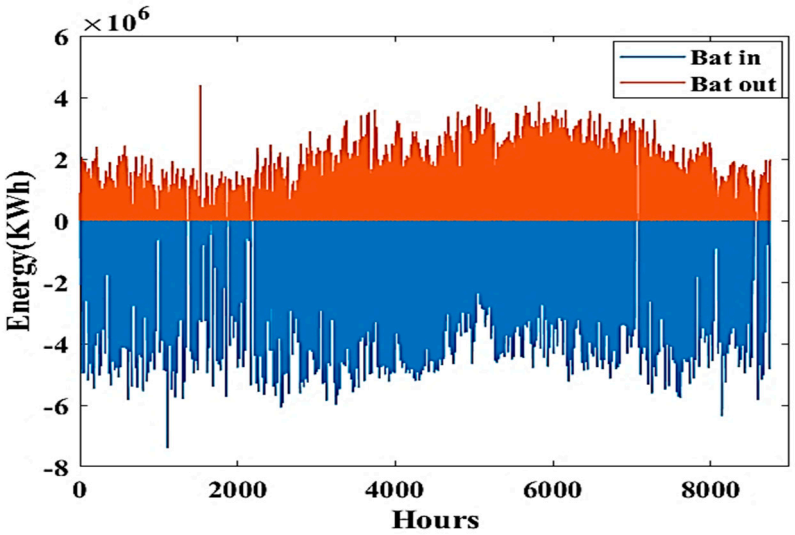

Figure 17. Annual battery input and output energy.

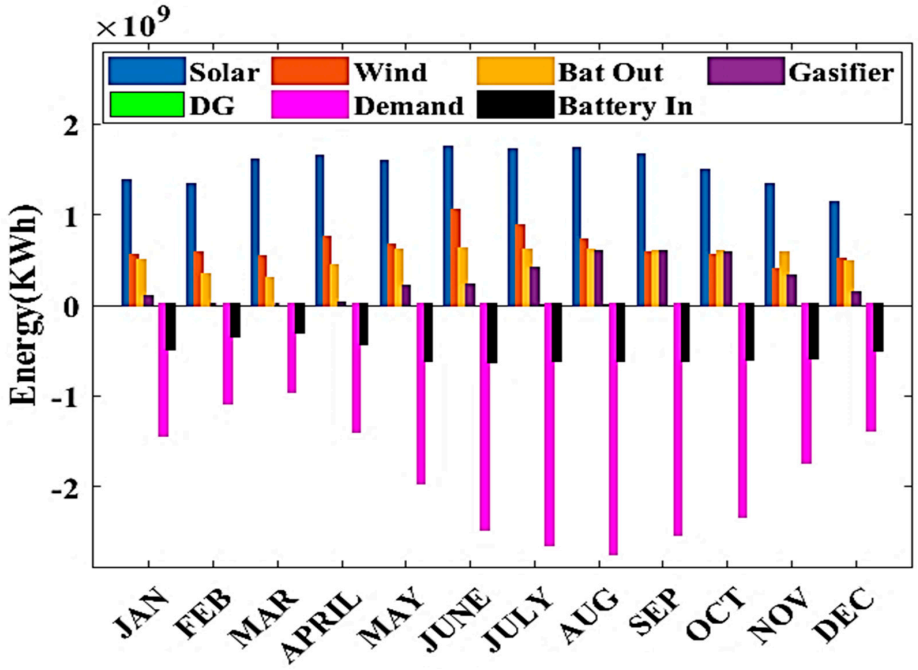

Figure 18. Annual monthly energy balance.

To ensure the proposed system would function optimally over a year, a period of one week has been selected for testing. For the purpose of illustrating the power flow throughout the system, Figure 19 illustrates a full power exchange for the first week of August (summer demand peaked here). As illustrated in the first day (Figure 20), the battery output (black curve) met the load demand between (4 h–6 h), (14 h–19 h), and (19 h–21 h), as solar and wind energy alone are insufficient to meet the deficit. Solar, wind, and battery energies were unable to meet the demand in the intervals (1 h–5 h), (5 h–7 h), (18 h–20 h) and (20 h–24 h) on the first day of August, so the bio-gasifier is adopted to meet the demand. Solar and wind power have been providing the day's other demand intervals without a doubt. All the adopted resources are insufficient to meet load by the end of the fifth day of this week, so the diesel generator is operating to do so as shown in Figure 21.

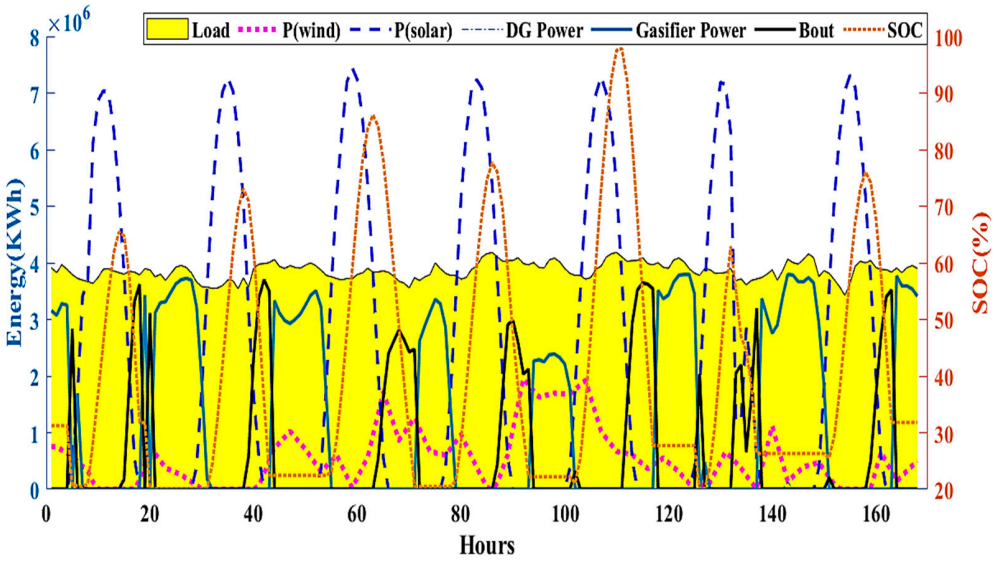

Figure 19. The power flow between adopted resources and demand in the first week of August.

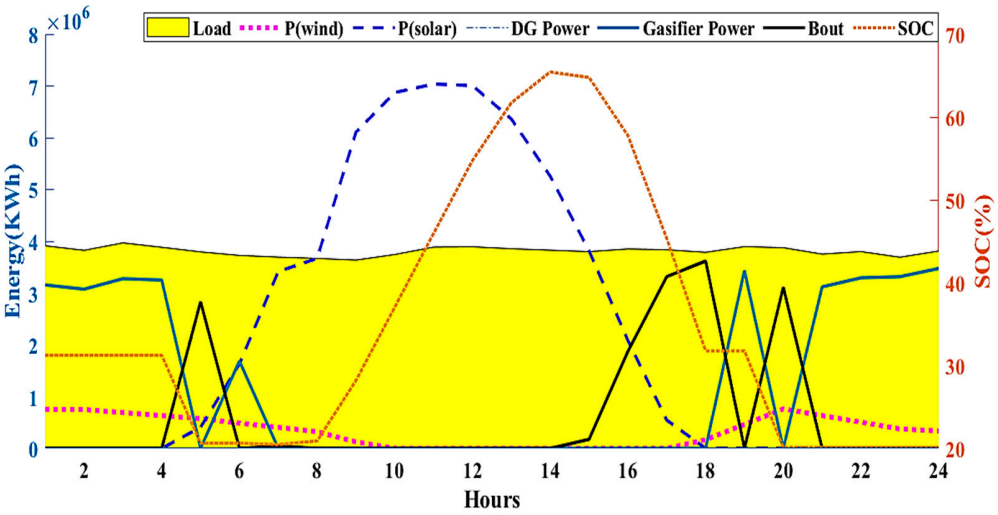

Figure 20. The power exchange between adopted resources and demand on the first day of August.

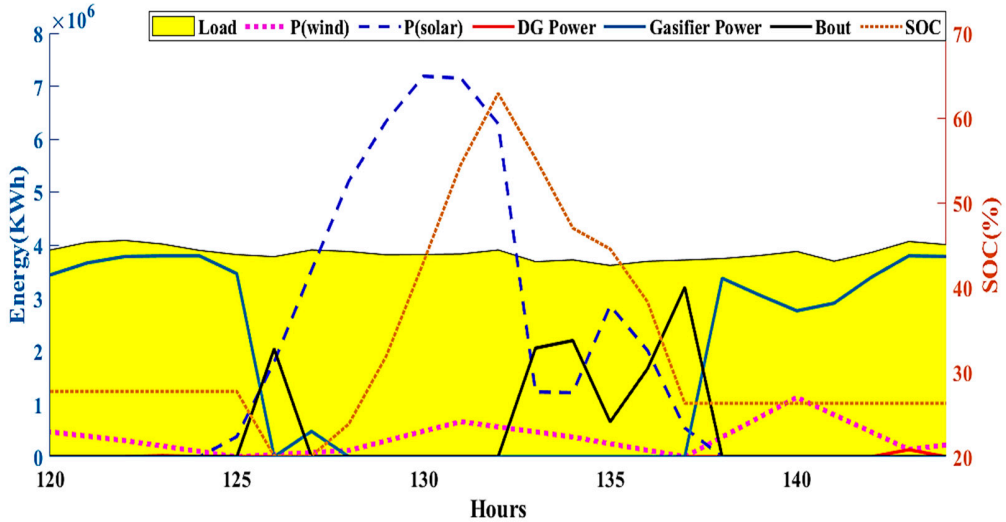

Figure 21. The power exchange between adopted resources and demand on the fifth day of August.

In systems employing batteries as storage devices, the measuring of SOC becomes crucial. Figure 22 shows the energy and average charge level of the battery bank for the first week of August. Initiating SOC is set at 100%, and the minimum acceptable SOC is set at 20%. In addition, as shown in Figure 22, battery SOC is good in most cases apart from when adopted resources are scarce or when load demand is high.

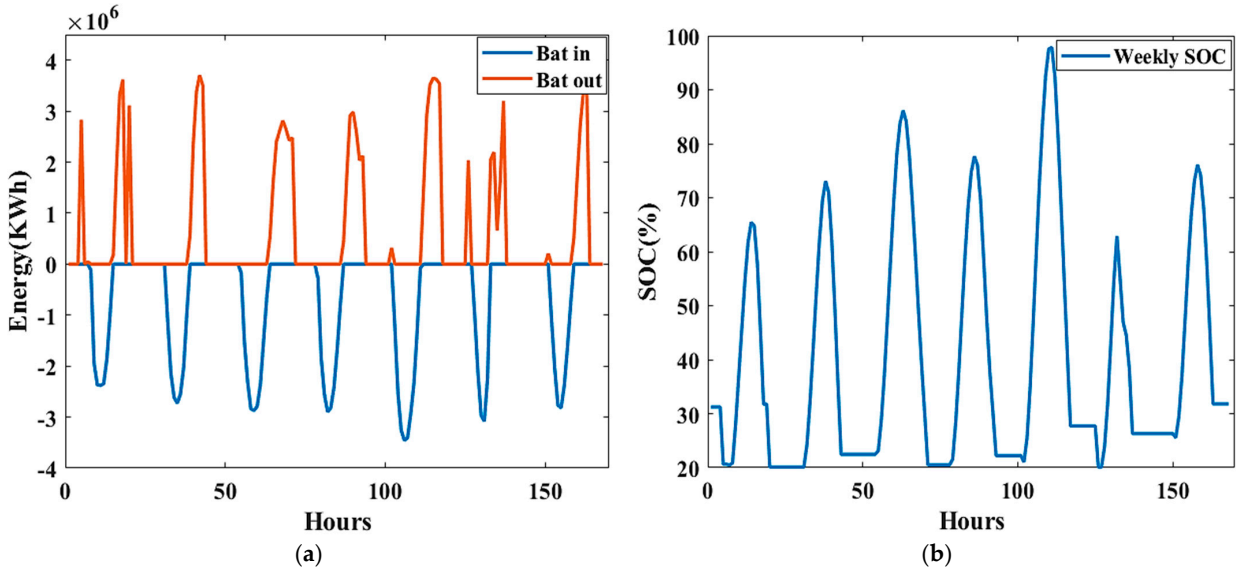

Figure 22. Battery SOC and energy of the first week in August. (**a**) Battery energy and (**b**) battery SOC.

The results for the first week of the month of January are shown in Figure 23 (as a winter case study). The load demand is low during the winter months. Wind and solar energies are adequate to meet the demand in the interval (5 h–15 h) of the first day of January, as shown in Figure 24. These energies alone are insufficient to meet the demand, so the battery output (black curve) fulfilled the load demand at all other intervals. The bio-gasifier has not been utilized in the majority of winter days because the load demand is low and can be satisfied by wind, solar, and storage energy. Figure 25 illustrates the energy and average charge level of the battery for the first week of January. The SOC of the battery is verified to be within the acceptable range, proving that the proposed method has been properly sized.

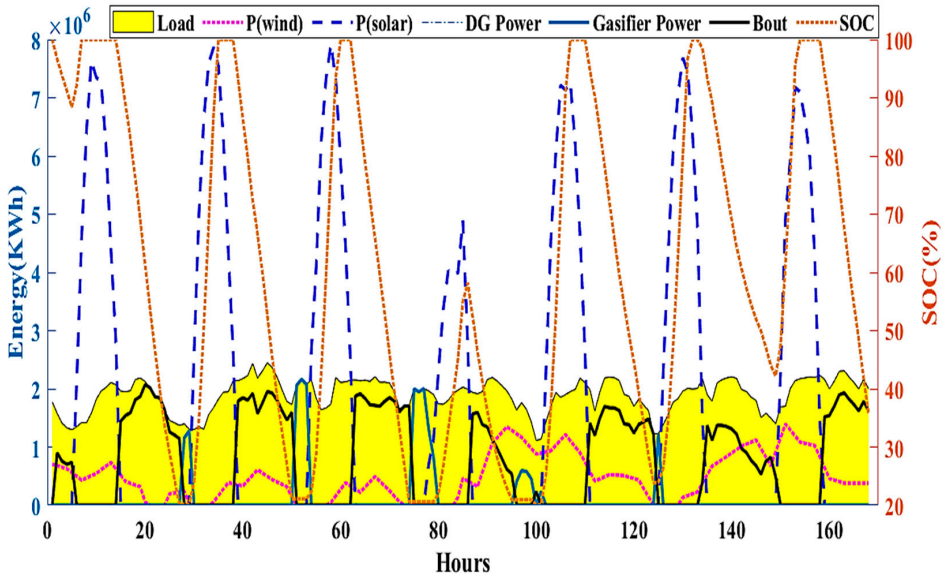

Figure 23. The power flow between adopted resources and demand in the first week of January.

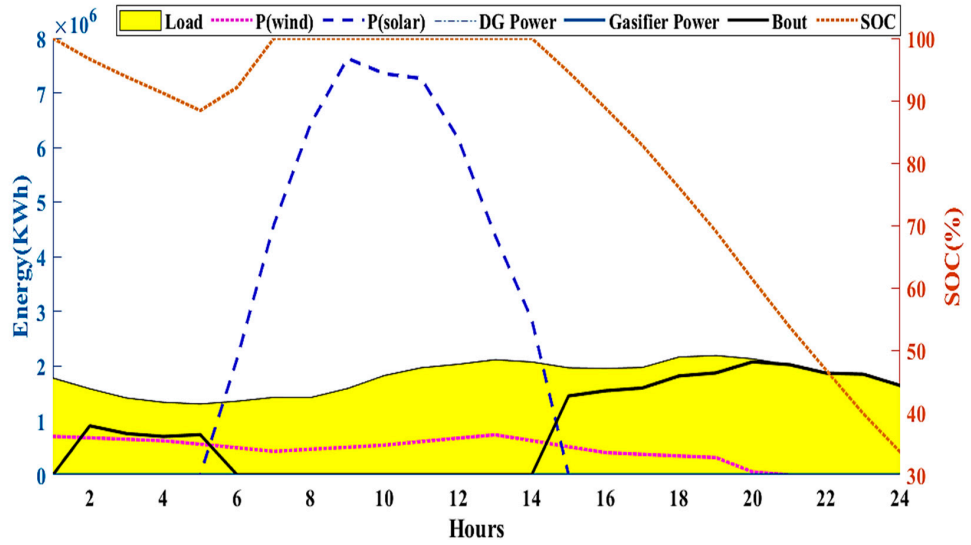

Figure 24. The power flow between adopted resources and demand on the first day of January.

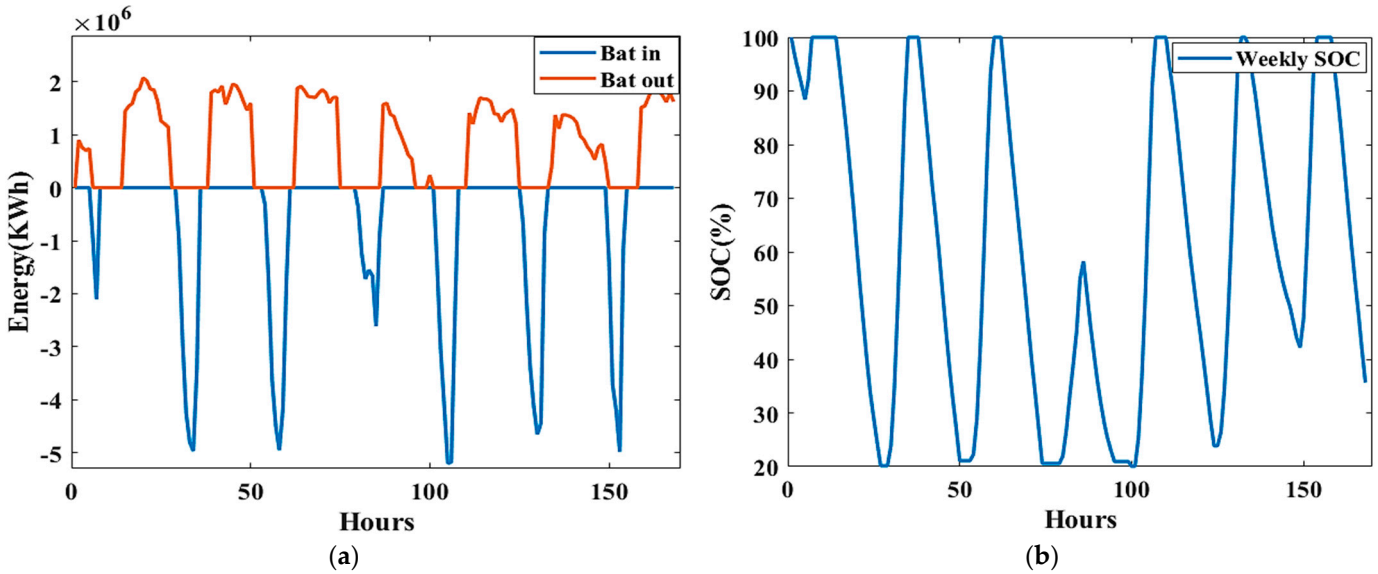

Figure 25. Battery SOC and energy of the first week in January. (**a**) Battery energy and (**b**) battery SOC.

7.3. Robustness and Speed Tests

Each algorithm has been independently run twenty times to establish its stability. Figure 26 shows the average and standard deviation of annual cost values. It is clear that the GWCSO algorithm is superior to other algorithms because it displays the lowest amount of deviation, leading to a small deviation from the mean. It is evident that GWCSO produces a lower mean value = 2.6963×10^9 and standard deviation = 9.23381×10^4. Figure 27 illustrates the computation time required by each algorithm to determine the optimal sizing of system components. The optimal solution can be found quickly with the GWO, GWCSO, and ALO algorithms, as contrasted to the other algorithms. The computation time for the GWO, GWCSO, and ALO is 403.3 s, 413.8 s, and 502.139 s, respectively. The results indicate that the GWCSO outperforms its competition in both robustness and speed.

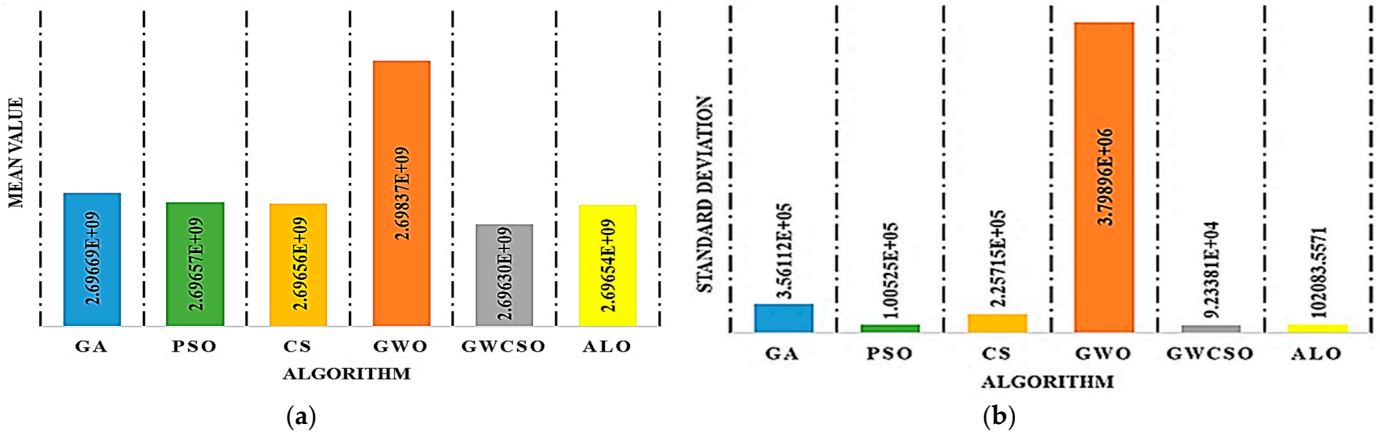

Figure 26. The annual (**a**) mean value of ANC and (**b**) standard deviation of the applied algorithms.

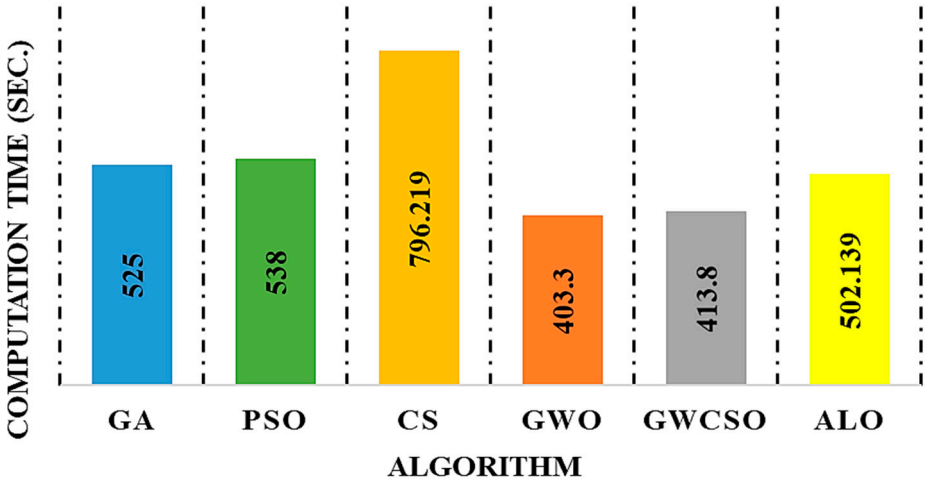

Figure 27. The processing times of the applied algorithms.

8. Conclusions

A method for calculating the optimal size of an energy management standalone MG system was proposed in this study. An integration of renewable and conventional sources, such as solar PV, WT, biomass gasifiers, diesel generators, and battery storage units, is used to power this system, which connects a DC bus and an AC bus using a power electronics conversion. The proposed hybrid MG system's primary objective is to provide the city of Basra, Iraq, with all the clean energy it requires, thereby eliminating the problems caused by the city's current grid, which include excessive fuel and operating costs, CO_2 emissions, and a centralized power structure. This paper proposes an optimization design based on a recently developed nature-inspired metaheuristic GWCSO optimization algorithm in order to find the lowest annual electricity costs with the fewest system component units. In the proposed energy management strategy, WT and solar PV renewable sources are prioritized for energy management, followed by energy storage units, then the biomass gasifier is adopted if the renewable and storage energies are insufficient to meet the demand; finally, the most expensive option, diesel generator, is used as a backup. This model takes into consideration resource coordination, system size, and component capacity. With this approach, the system can engage in energy trading and investment. To demonstrate the validity and efficacy of the proposed method utilizing GWCSO, simulations based on actual weather data gathered from the study site have been conducted. The results of the proposed energy management system based on the GWCSO algorithm have been compared to those of the PSO, GA, CS, GWO, and ALO. The results indicate that the GWCSO algorithm

is capable of determining the lowest LCOE, costs, and minimum number of component units for the system. According to the results, GWCSO generates the lowest ANC value (2.6918×10^9), followed by PSO and ALO (2.6919×10^9 and 2.6923×10^9, respectively). These three algorithms yield a LCOE of 0.1192. The proposed algorithm also outperformed others in terms of robustness, as its deviation over multiple runs was lower (9.23381×10^4).

In the future, we will research recent optimization techniques to further reduce the system components, annual cost, and LCOE. To enhance the load factor and optimize load supply, a demand-side management program might be incorporated for future research. Additionally, the impact of transmission packet losses on a supply–demand mismatch can be added and studied.

Author Contributions: Authors: A.M.J.: original draft, software, methodology, and validation; B.H.J.: supervisor, formal analysis; research resources; investigation; editing; and writing; F.-C.B.: editing; formal analysis; validation; B.-C.N.; visualization; formal analysis; project administration; funding acquisition. All authors have read and agreed to the published version of the manuscript.

Funding: This research was funded by national grant PN III PFE, project no. 27PFE/2021, COMPETE 2.0 (Gheorghe Asachi Technical University of Iasi), financed by the Romanian Government.

Data Availability Statement: Not applicable.

Conflicts of Interest: The authors declare no conflict of interest.

References

1. Jasim, A.M.; Jasim, B.H.; Neagu, B.-C.; Alhasnawi, B.N. Efficient Optimization Algorithm-Based Demand-Side Management Program for Smart Grid Residential Load. *Axioms* **2023**, *12*, 33. [CrossRef]
2. Jasim, A.M.; Jasim, B.H.; Kraiem, H.; Flah, A. A Multi-Objective Demand/Generation Scheduling Model-Based Microgrid Energy Management System. *Sustainability* **2022**, *14*, 10158. [CrossRef]
3. Haratian, M.; Tabibi, P.; Sadeghi, M.; Vaseghi, B.; Poustdouz, A. A renewable energy solution for stand-alone power generation: A case study of KhshU Site-Iran. *Renew Energy* **2018**, *125*, 926–935. [CrossRef]
4. Heydari, A.; Askarzadeh, A. Optimization of a biomass-based photovoltaic power plant for an off-grid application subject to loss of power supply probability concept. *Appl. Energy* **2016**, *165*, 601–611. [CrossRef]
5. Jasim, A.M.; Jasim, B.H.; Bureš, V.; Mikulecký, P. A New Decentralized Robust Secondary Control for Smart Islanded Microgrids. *Sensors* **2022**, *22*, 8709. [CrossRef]
6. Alhasnawi, B.N.; Jasim, B.H.; Sedhom, B.E.; Guerrero, J.M. Consensus Algorithm-based Coalition Game Theory for Demand Management Scheme in Smart Microgrid. *Sustain. Cities Soc.* **2017**, *74*, 103248. [CrossRef]
7. Alhasnawi, B.N.; Jasim, B.H.; Alhasnawi, A.N.; Sedhom, B.E.; Jasim, A.M.; Khalili, A.; Bureš, V.; Burgio, A.; Siano, P. A Novel Approach to Achieve MPPT for Photovoltaic System Based SCADA. *Energies* **2022**, *15*, 8480. [CrossRef]
8. Almusawi, H.M.; Farnoosh, A. Economic Analysis of the Electricity Mix of Iraq using Portfolio Optimization Approach. *Int. Energy J.* **2021**, *21*, 235–2445.
9. Available online: https://dateandtime.info/citycoordinates.php?id=99532. (accessed on 7 February 2023).
10. Chaichan, M.T.; Abass, K.I.; Kazem, H.A. Energy yield loss caused by dust and pollutants deposition on concentrated solar power plants in Iraq weathers. *Int. Res. J. Adv. Eng. Sci.* **2018**, *3*, 160–169.
11. Chaichan, M.T.; Kazem, H.A. *Generating Electricity Using Photovoltaic Solar Plants in Iraq*; Springer International Publishing: Cham, Switzerland, 2018. [CrossRef]
12. Alasady, A.M.A. Solar energy the suitable energy alternative for Iraq beyond oil. In *Proceedings of the International Conference on Petroleum and Sustainable Development (IPCBEE)*; IACSIT Press: Singapore, 2011; Volume 26, pp. 11–15.
13. Darwish, A.S.K.; Sayigh, A.A.M. Wind energy potential in Iraq. *Sol. Wind Technol.* **1988**, *5*, 215–222. [CrossRef]
14. Dihrab, S.S.; Sopian, K. Electricity generation of hybrid PV/wind systems in Iraq. *Renew. Energy* **2010**, *35*, 1303–1307. [CrossRef]
15. Abed, F.M.; Al-Douri, Y.; Al-Shahery, G. Review on the energy and renewable energy status in Iraq: The outlooks. *Renew. Sustain. Energy Rev.* **2014**, *39*, 816–827. [CrossRef]
16. Jasim, A.M.; Jasim, B.H.; Neagu, B.-C. A New Decentralized PQ Control for Parallel Inverters in Grid-Tied Microgrids Propelled by SMC-Based Buck–Boost Converters. *Electronics* **2022**, *11*, 3917. [CrossRef]
17. Ahamad, N.B.; Othman, M.; Vasquez, J.C.; Guerrero, J.M.; Su, C.L. Optimal sizing and performance evaluation of a renewable energy based microgrid in future seaports. In Proceedings of the 2018 IEEE International Conference on Industrial Technology (ICIT), Lyon, France, 20–22 February 2018; pp. 1043–1048.
18. Oviedo, J.; Duarte, C.; Solano, J. Sizing of Hybrid Islanded Microgrids using a Heuristic approximation of the Gradient Descent Method for discrete functions. *Int. J. Renew. Energy Res.* **2020**, *10*, 13–22.

19. Bukar, A.L.; Tan, C.W.; Lau, K.Y. Optimal sizing of an autonomous photovoltaic/wind/battery/diesel generator microgrid using grasshopper optimization algorithm. *Sol. Energy* **2019**, *188*, 685–696. [CrossRef]
20. Zhang, W.; Maleki, A.; Rosen, M.A.; Liu, J. Sizing a stand-alone solar-wind-hydrogen energy system using weather forecasting and a hybrid search optimization algorithm. *Energy Convers. Manag.* **2019**, *180*, 609–621. [CrossRef]
21. Giallanza, A.; Porretto, M.; Puma, G.L.; Marannano, G. A sizing approach for stand-alone hybrid photovoltaic-windbattery systems: A Sicilian case study. *J. Clean. Prod.* **2018**, *199*, 817–830. [CrossRef]
22. Rullo, P.; Braccia, L.; Luppi, P.; Zumoffen, D.; Feroldi, D. Integration of sizing and energy management based on economic predictive control for standalone hybrid renewable energy systems. *Renew. Energy* **2019**, *140*, 436–451. [CrossRef]
23. Tabak, A.; Kayabasi, E.; Guneser, M.T.; Ozkaymak, M. Grey wolf optimization for optimum sizing and controlling of a PV/WT/BM hybrid energy system considering TNPC, LPSP, and LCOE concepts. *Energy Sources Part A Recovery Util. Environ. Eff.* **2019**, *44*, 1508–1528. [CrossRef]
24. Farh, H.M.; Al-Shamma'a, A.A.; Al-Shaalan, A.M.; Alkuhayli, A.; Noman, A.M.; Kandil, T. Technical and economic evaluation for off-grid hybrid renewable energy system using novel Bonobo optimizer. *Sustainability* **2022**, *14*, 1533. [CrossRef]
25. Alshammari, S.; Fathy, A. Optimum Size of Hybrid Renewable Energy System to Supply the Electrical Loads of the Northeastern Sector in the Kingdom of Saudi Arabia. *Sustainability* **2022**, *14*, 13274. [CrossRef]
26. Aziz, A.; Tajuddin, M.; Adzman, M.; Ramli, M.; Mekhilef, S. Energy Management and Optimization of a PV/Diesel/Battery Hybrid Energy System Using a Combined Dispatch Strategy. *Sustainability* **2019**, *11*, 683. [CrossRef]
27. Jayachandran, M.; Ravi, G. Design and optimization of hybrid micro-grid system. *Energy Procedia* **2017**, *117*, 95–103. [CrossRef]
28. Salawudeen, A.T.; Mu'azu, M.B.; Sha'aban, Y.A.; Adedokun, A.E. A Novel Smell Agent Optimization (SAO): An extensive CEC study and engineering application. *Knowl.-Based Syst.* **2021**, *232*, 107486. [CrossRef]
29. Rezk, H.; Al-Dhaifallah, M.; Hassan, Y.B.; Ziedan, H.A. Optimization and Energy Management of Hybrid Photovoltaic-Diesel Battery System to Pump and Desalinate Water at Isolated Regions. *IEEE Access* **2020**, *8*, 102512–102529. [CrossRef]
30. Tran, Q.T.; Davies, K.; Sepasi, S. Isolation Microgrid Design for Remote Areas with the Integration of Renewable Energy: A Case Study of Con Dao Island in Vietnam. *Clean Technol.* **2021**, *3*, 804–820. [CrossRef]
31. Lu, X.; Wang, H. Optimal sizing and energy management for cost-effective PEV hybrid energy storage systems. *IEEE Trans. Ind. Inform.* **2019**, *16*, 3407–3416. [CrossRef]
32. Diab, A.A.Z.; Sultan, H.M.; Mohamed, I.S.; Kuznetsov, O.N.; Do, T.D. Application of different optimization algorithms for optimal sizing of PV/wind/diesel/battery storage stand-alone hybrid microgrid. *IEEE Access* **2019**, *7*, 119223–119245. [CrossRef]
33. Acevedo-Arenas, C.Y.; Correcher, A.; Sánchez-Díaz, C.; Ariza, E.; Alfonso-Solar, D.; Vargas-Salgado, C.; Petit-Suárez, J.F. MPC for optimal dispatch of an AC-linked hybrid PV/wind/biomass/H2 system incorporating demand response. *Energy Convers. Manag.* **2019**, *186*, 241–257. [CrossRef]
34. Diab, A.A.Z.; El-Rifaie, A.M.; Zaky, M.M.; Tolba, M.A. Optimal Sizing of Stand-Alone Microgrids Based on Recent Metaheuristic Algorithms. *Mathematics* **2022**, *10*, 140. [CrossRef]
35. Zhu, X.; Premrudeepreechacharn, S.; Sorndit, C.; Meenual, T.; Kasirawat, T.; Tantichayakorn, N. Design and Development of a Microgrid Project at Rural Area. In Proceedings of the 2019 IEEE PES GTD Grand International Conference and Exposition Asia (GTD Asia), Bangkok, Thailand, 19–23 March 2019; pp. 877–882.
36. Bakar, N.N.A.; Guerrero, J.M.; Vasquez, J.C.; Bazmohammadi, N.; Othman, M.; Rasmussen, B.D.; Al-Turki, Y.A. Optimal Configuration and Sizing of Seaport Microgrids including Renewable Energy and Cold Ironing-The Port of Aalborg Case Study. *Energies* **2022**, *15*, 431. [CrossRef]
37. Yasin, A.; Alsayed, M. Optimization with excess electricity management of a PV, energy storage and diesel generatorhybrid system usingHOMER Pro software. *Int. J. Appl. Power Eng.* **2020**, *9*, 267–283, ISSN: 2252–8792. [CrossRef]
38. Shahzad, M.; Zahid, A.; Rashid, T.; Rehan, M.; Ali, M.; Ahmad, M. Techno-economic feasibility analysis of a solar-biomass off grid system for electrification of remote rural areas in Pakistan using HOMER software. *Renew. Energy* **2017**, *106*, 264–273. [CrossRef]
39. Zahboune, H.; Zouggar, S.; Krajacic, G.; Varbanov, P.; Elhafyani, M.; Ziani, E. Optimal hybrid renewable energy design in autonomous system using modified electric system cascade analysis and HOMER software. *Energy Convers. Manag.* **2022**, *126*, 909–922. [CrossRef]
40. Halabi, L.; Mekhilef, S.; Olatomiwa, L.; Hazelton, J. Performance analysis of hybrid PV/diesel/battery system using HOMER: A case study Sabah, Malaysia. *Energy Convers Manag.* **2017**, *144*, 322–339. [CrossRef]
41. Abu-Hijleh, B. Use of hybrid PV and wind turbine-grid connected system in a local Emirati home in Dubai-UAE. *Energy Procedia* **2016**, *100*, 463–468. [CrossRef]
42. Das, B.K.; Zaman, F. Performance Analysis of a PV/Diesel Hybrid System for a Remote Area in Bangladesh: Effects of Dispatch Strategies, Batteries, and Generator Selection. *Energy* **2018**, *169*, 263–276. [CrossRef]
43. Yenalem, M.G.; Shiferaw, D.; Hinga, P. Modelling and Optimal Sizing of Grid-Connected Micro grid System using HOMER in Bahir Dar City, Ethiopia. *Int. J. Power Syst.* **2020**, *5*, 1–12.
44. Kumar, S.; Kaur, T.; Arora, M.K.; Upadhyay, S. Resource estimation and sizing optimization of PV/micro hydro-based hybrid energy system in rural area of Western Himalayan Himachal Pradesh in India. *Energy Sources Part A* **2019**, *41*, 2795–2807. [CrossRef]
45. Mukasa, A.D.; Mutambatsere, D.; Arvanitis, Y.; Triki, T. *Development of Wind Energy in Africa*; Working Paper Series N° 170; African Development Bank: Tunis, Tunisia, 2013.

46. Mirza, Z.T.; Mehrdad Abedi, B.V. Renewable Energy Development in India & Iran: A Comparative Review of Renewable Energy Policies. *Am. J. Energy Eng.* **2022**, *10*, 21–34. [CrossRef]
47. Makkiabadi, M.; Hoseinzadeh, S.; Taghavirashidizadeh, A.; Soleimaninezhad, M.; Kamyabi, M.; Hajabdollahi, H.; Nezhad, M.M.; Piras, G. Performance Evaluation of Solar Power Plants: A Review and a Case Study. *Processes* **2021**, *9*, 2253. [CrossRef]
48. Available online: https://www.power-eng.com/renewables/midamerican-plans-to-add-2-gw-of-wind-energy-resources-in-iowa/#gref (accessed on 12 November 2022).
49. Erdin, C.; Ozkaya, G. Turkey's 2023 Energy Strategies and Investment Opportunities for Renewable Energy Sources: Site Selection Based on ELECTRE. *Sustainability* **2019**, *11*, 2136. [CrossRef]
50. Han, M.; Tang, J.; Lashari, A.K.; Abbas, K.; Liu, H.; Liu, W. Unveiling China's Overseas Photovoltaic Power Stations in Pakistan under Low-Carbon Transition. *Land* **2022**, *11*, 1719. [CrossRef]
51. Dubai Electricity and Water Authority. Available online: https://www.dewa.gov.ae/en/ (accessed on 15 November 2022).
52. Ramachandran, T.; Abdel-Hamid, I.M.; Hamed, F. A Review on Solar Energy Utilization and Projects: Development in and around the UAE. *Energies* **2022**, *15*, 3754. [CrossRef]
53. Available online: https://en.wikipedia.org/wiki/List_of_power_stations_in_Iraq (accessed on 3 January 2023).
54. Ali, M.J.; Basil, H.J.; Flah, A.; Hossam, K.; Ahmed, A. Consensus-Based Intelligent Distributed Secondary Control for Multiagent Islanded Microgrid. *Int. Trans. Electr. Energy Syst.* **2023**, *2023*, 1–20. [CrossRef]
55. Ali, M.J.; Basil, H.J.; Soheil, M.; Alan, C.B. Consensus-Based Dispatch Optimization of a Microgrid Considering Meta-Heuristic-Based Demand Response Scheduling and Network Packet Loss Characterization. *Energy AI* **2022**, *11*, 100212. [CrossRef]
56. Hamrouni, N.; Jraidi, M. Chérif, a Solar radiation and ambient temperature effects on the performances of a PV pumping system. *Rev. Energ. Renouvelables* **2008**, *11*, 95–106.
57. Sukamongkol, Y.; Chungpaibulpatana, S.; Ongsakul, W. A simulation model for predicting the performance of a solar photovoltaic system with alternating current loads. *Renew. Energy* **2002**, *27*, 237–258. [CrossRef]
58. Singh, S.; Singh, M.; Kaushik, S.C. Feasibility study of an islanded microgrid in rural area consisting of PV, wind, biomass and battery energy storage system. *Energy Convers. Manag.* **2016**, *128*, 178–190. [CrossRef]
59. Jasim, A.M.; Jasim, B.H.; Bureš, V. A novel grid-connected microgrid energy management system with optimal sizing using hybrid grey wolf and cuckoo search optimization algorithm. *Front. Energy Res.* **2022**, *10*, 960141. [CrossRef]
60. Jasim, A.M.; Jasim, B.H.; Neagu, B.-C.; Alhasnawi, B.N. Coordination Control of a Hybrid AC/DC Smart Microgrid with Online Fault Detection, Diagnostics, and Localization Using Artificial Neural Networks. *Electronics* **2023**, *12*, 187. [CrossRef]
61. Skarstein, O.; Uhlen, K. Design considerations with respect to long-term diesel saving in wind/diesel plants. *Wind Eng.* **1989**, *13*, 72–87.
62. Azoumah, Y.; Yamegueu, D.; Ginies, P.; Coulibaly, Y.; Girard, P. Sustainable electricity generation for rural and peri-urban populations of sub-Saharan Africa: The "flexy-energy" concept. *Energy Policy* **2011**, *39*, 131–141. [CrossRef]
63. Qari, H.; Khosrogorji, S.; Torkaman, H. Optimal sizing of hybrid WT/PV/diesel generator/battery system using MINLP method for a region in Kerman. *Sci. Iran.* **2020**, *27*, 3066–3074. [CrossRef]
64. Xu, H.; Liu, X.; Su, J. An improved grey wolf optimizer algorithm integrated with Cuckoo Search. In Proceedings of the 2017 9th IEEE International Conference on Intelligent Data Acquisition and Advanced Computing Systems: Technology and Applications (IDAACS), Bucharest, Romania, 21–23 September 2017. [CrossRef]
65. Alhasnawi, B.N.; Jasim, B.H.; Rahman, Z.-A.S.A.; Siano, P. A Novel Robust Smart Energy Management and Demand Reduction for Smart Homes Based on Internet of Energy. *Sensors* **2021**, *21*, 4756. [CrossRef] [PubMed]
66. Cuevas, E.; Reyna-Orta, A. A Cuckoo Search Algorithm for Multimodal Optimization. *Hindawi Publ. Corp. Sci. World J.* **2014**, *2014*, 497514. [CrossRef] [PubMed]
67. Mudgal, V.; Singh, P.; Khanna, S.; Pandey, C.; Becerra, V.; Mallick, T.K.; Reddy, K.S. Optimization of a novel Hybrid Wind Bio Battery Solar Photovoltaic System Integrated with Phase Change Material. *Energies* **2021**, *14*, 6373. [CrossRef]
68. Belboul, Z.; Toual, B.; Kouzou, A.; Mokrani, L.; Bensalem, A.; Kennel, R.; Abdelrahem, M. Multiobjective Optimization of a Hybrid PV/Wind/Battery/Diesel Generator System Integrated in Microgrid: A Case Study in Djelfa, Algeria. *Energies* **2022**, *15*, 3579. [CrossRef]
69. Ali, M.J.; Basil, H.J.; Vladimir, B.; Mikulecky, P. A Novel Cooperative Control Technique for Hybrid AC/DC Smart Microgrid Converters. *IEEE Access* **2023**, *11*, 2164–2181. [CrossRef]
70. Available online: https://re.jrc.ec.europa.eu/pvg_tools/en/# (accessed on 3 January 2023).